

Brown
1987
23

GEOLOGY OF THE SOUTHERN CAÑONCITO DE LA UVA AREA,
SOCORRO COUNTY, NEW MEXICO

by

Karen B. Brown

LIBRARY
SOCORRO, N.M.

Submitted as partial fulfillment of the requirements
for a Master of Science degree in Geology

New Mexico Institute of Mining and Technology

15 April, 1987

File 44

ABSTRACT

Cañoncito de la Uva, in central Socorro County on the east edge of the Rio Grande rift, exposes Paleozoic rocks with structural features that are assigned to several time periods. Pennsylvanian Burrego, Story, Del Cuerto, and Moya Formations represent marine deposition. Regression and influx of clastic sediments began with Permian Bursum deposition, and reached a climax as the fluviatile Abo Formation was deposited. Rapid facies and thickness changes in these strata are a result of penecontemporaneous tectonic movement. Yeso sandstone, limestone and gypsum indicate a return of marine conditions.

The marine and nonmarine sediments are distorted by several tectonic episodes. Major structures of the area include north-northwest trending open and isoclinal folds with eastward vergence, north-northwest striking high and low angle reverse faults, and north-northwest striking normal faults. Northerly trending zones of anastomosing fault splays with minor offset on individual faults, northeast trending faults with changes of dip direction, and northeast trending fold axes are of lesser significance. At least three periods of deformation are represented.

The first structural deformation created local uplifts and basins during deposition of Pennsylvanian and some Permian strata. Some faults of this period may be present in the area. The second tectonic event to affect the area occurred after deposition of the Paleozoic sediments was complete. The Montosa fault, a northeast-trending, right-lateral wrench structure, enters the north edge of the field area, and becomes obscure to non-existent in less than one half of a kilometer. A major uplift of folded and overturned Pennsylvanian strata occurs southwest of the termination, striking across the trend of the Montosa fault. Thrust and high-angle reverse faults strike parallel to the fold axes. Another northeast-trending, right-lateral wrench fault is present to the southwest of the field area, parallel to but off trend from, the Montosa fault. This fault terminates near the southern end of the uplift. This folding, uplift and thrusting is a result of compressional forces between terminations of the two right-lateral wrench faults. High-angle, normal faults associated with opening of the Rio Grande rift cut the earlier structures.

TABLE OF CONTENTS

ABSTRACT	i
TABLE OF CONTENTS	iii
LIST OF FIGURES	v
LIST OF PLATES	viii
INTRODUCTION	1
Purpose of Study	1
Location and Extent	1
Field Methods	3
Previous Work	4
Acknowledgements	5
STRATIGRAPHY	7
Description of Units	9
Council Spring Limestone	9
Burrego Formation	9
Story Formation	11
Del Cuerto Formation	12
Moya Formation	13
Bursum Formation	19
Abo Formation	20
Yeso Formation	24
DEPOSITIONAL HISTORY	28
STRUCTURAL GEOLOGY	33
Description of Structures	40
Faults	40
Folds	48

Regional and Comparative Structure	51
Structural Discussion	68
APPENDIX OF TABLES	77
Table 1. Thin Section Descriptions	78
Table 2. Fault Plane Attitudes	83
Table 3. Fold Axes	84
REFERENCES CITED	85

LIST OF FIGURES

<u>FIGURE</u>	<u>CAPTION</u>	<u>PAGE</u>
1:	Location map and physiographic features of the southern Cañoncito de la Uva area.	2
2:	Pennsylvanian stratigraphic nomenclature in central New Mexico, from Thompson, 1942, Table II, p. 27.	8
3:	Intraclast breccia in Moya Formation	15
4:	Crossbedded crinoidal grainstones in Moya Formation	16
5:	Stylolite detail in Moya Formation	17
6:	Convoluted sandstone bed in Moya Formation	18
7:	Bursum Formation exposures in s. 14.	21
8:	Westward from east ridge: Abo exposures in middle-ground, Bursum at the base of the slope on both sides of the wash.	23
9:	Discoloration of beds in Meseta Blance Member, view northeast from Baca well.	26
10:	Drag folds on fault, s. 9, view northeast, Bursum Formation.	34
11:	Abo Formation, foliation imparted, compass points north, s. 23.	35
12:	Torres Member, breccia dike in channel, s. 13.	36
13:	Abo Formation, intersecting breccia dikes, s. 9.	37
14:	Abo Formation, cataclastic texture, compass points north, s. 24.	38
15:	Moya Formation, right-stepping extensional fractures in s. 16.	39
16:	Structural features of the Cañoncito de la Uva area	41
17:	STEREOGRAPH OF CLASS I AND II FAULTS	43
18:	STEREOGRAPH OF CLASS III, IV, V FAULTS	44

<u>FIGURE</u>	<u>CAPTION</u>	<u>PAGE</u>
19:	Abo Formation juxtaposed against Pennsylvanian rocks on normal fault, s. 20, view north-northwest; Burrego, Story, Del Cuerto, and Moya Formations exposed in grey slope to right of Red Abo	45
20:	Small, low-angle reverse fault in central ridge	47
21:	FOLD AXES STEREOGRAPH	49
22:	Cross section through incipient horses. New fractures (dashed) may cut horses from either footwall of hanging wall of major thrust surface. Strata of horse need not be overturned as this diagram shows. From Boyer and Elliott, 1982, figure 9, p. 1199.	53
23:	Cross section of imbricate thrust sheets, which merge asymptotically downward to a common basal sole thrust. From Boyer and Elliott, 1982, figure 11, p. 1199.	55
24:	Cross section of Rio Grande uplift in the southeastern Caballo Mountains. From Seager, 1986, figure 7, p. 128.	56
25:	a) Overthrust due to compression b) Upthrust due to differential vertical uplift. From Hafner, 1958, figure 2, p. 2.	58
26:	Positive flower structure produced in a transpressive wrench regime (after Harding, 1985, p. 593).	59
27:	Types of strike-slip fault patterns, which produce subsided basins and uplifted blocks. From Reading, 1980, figure 3, p. 12.	60
28:	Strain ellipse in a right-lateral wrench regime: R, P, Y: synthetic wrench faults and wrench zone R1, X: antithetic strike-slip faults. Fold axes in direction of elongation of strain ellipse. From Hancock, 1985; "loosely after" Harding, 1974.	62

<u>FIGURE</u>	<u>CAPTION</u>	<u>PAGE</u>
29:	Conceptual diagram of an upthrust-bounded welt created by convergent strike-slip motion. Low convergence angle causes each segment to move a small distance past the next in a right-slip direction. The space problem created is relieved by upward movement. Deeper faults may tend to coalesce and braid, rather than be parallel, and the upthrusts are not so symmetrically disposed as is shown. From Lowell, 1972, figure 9, p. 3099.	63
30:	COCORP seismic sections which traverse the rift. VP spacing for line 1A is 134 m; line 1, 100 m. Location map of the lines shown at upper left. From Brown et al., 1979, figures 1 and 3, p. 171 and 175.	65
31:	Generalized map of the Rio Grande rift and major crustal lineaments. From Chapin et al., 1978, figure 1, p. 114.	67
32:	Diagram of wrench faults terminating at the ends of the compressional central ridge. Note the location of splays with small offset to the east of the folded area. Normal faulting after development of this structure has led to this exposure.	69
33:	Possible allochthonous origin of the central compressional ridge.	71
34:	Horst interpretation of the central ridge.	72
35:	Diagram of possible regional relations from Abo Pass, southward through Cañoncito de la Uva area.	75

LIST OF PLATES

<u>PLATE</u>		<u>LOCATION</u>
1	Geologic Map of the Cañoncito de la Uva Area	in pocket
2	East-west Geologic Cross Sections	in pocket
3	Northwest-southeast Geologic Cross Sections	in pocket
4	Small Geologic Cross Sections Through Central Ridge	in pocket
5	Explanation of Geologic Cross Sections	in pocket
6	Explanation of Stratigraphic Columns	in pocket
7	Stratigraphic Column of Burrego Formation	in pocket
8	Stratigraphic Column of Story through Moya Formations	in pocket
9	Stratigraphic Column of Moya Formation	in pocket
10	Stratigraphic Column of Moya Formation	in pocket
11	Stratigraphic Column of Bursam Formation	in pocket
12	Stratigraphic Column of Abo Formation	in pocket

INTRODUCTION

Purpose of Study

This field study was undertaken to continue documentation of tectonic features in the Rio Grande rift region. The nature of the regional structure in the Rio Grande rift area prior to rifting is not well understood, in part because extensional tectonics associated with rifting has obscured pre-rift features. It is hoped this small portion of detailed mapping in the southern Los Piños Mountains can enhance regional interpretation and understanding of geologic features in central New Mexico.

Location and Extent

The Cañoncito de la Uva area is in the southernmost Los Piños Mountains, in central New Mexico, about 24 kilometers (15 miles) from Socorro, 13 kilometers (8 miles) east of the Rio Grande. The area mapped lies in township 2 north, range 2 east, and covers all or parts of sections 8 through 16, and 21 through 29 (longitude $106^{\circ} 40' W.$ to $106^{\circ} 45' W.$, latitude $34^{\circ} 6' 26'' N.$ to $34^{\circ} 8' 30'' N.$). Figure 1 shows local and regional topographic features and location.

The topographic expression of the Los Piños Mountains is not as sharply defined here as it is further north. At the latitude of Cañoncito de la Uva,

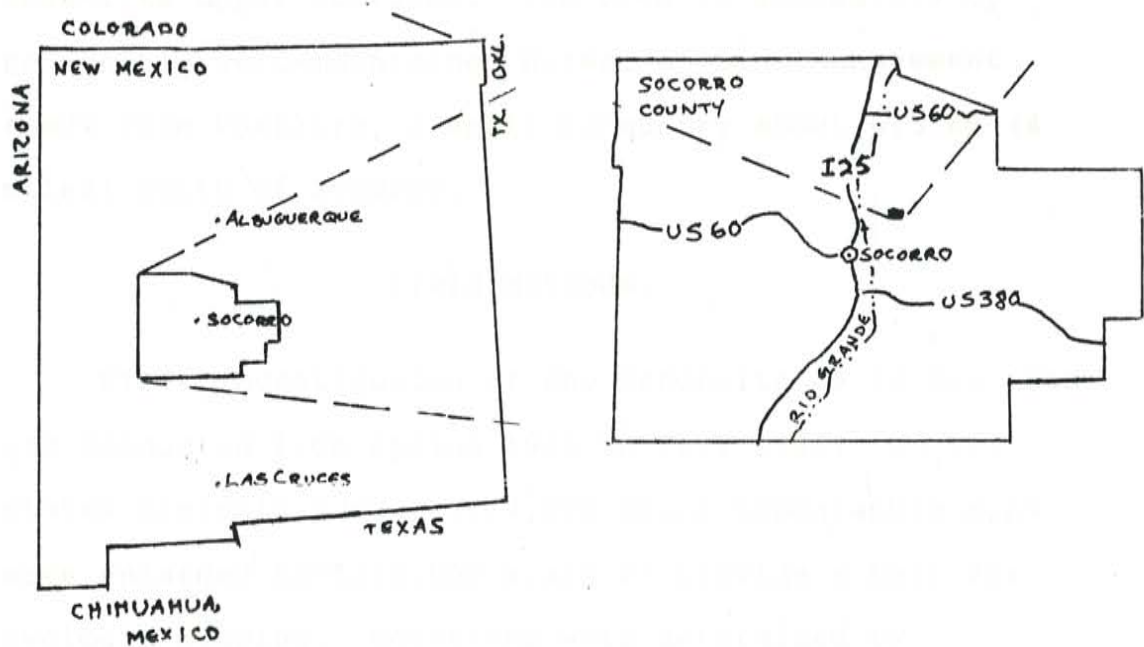
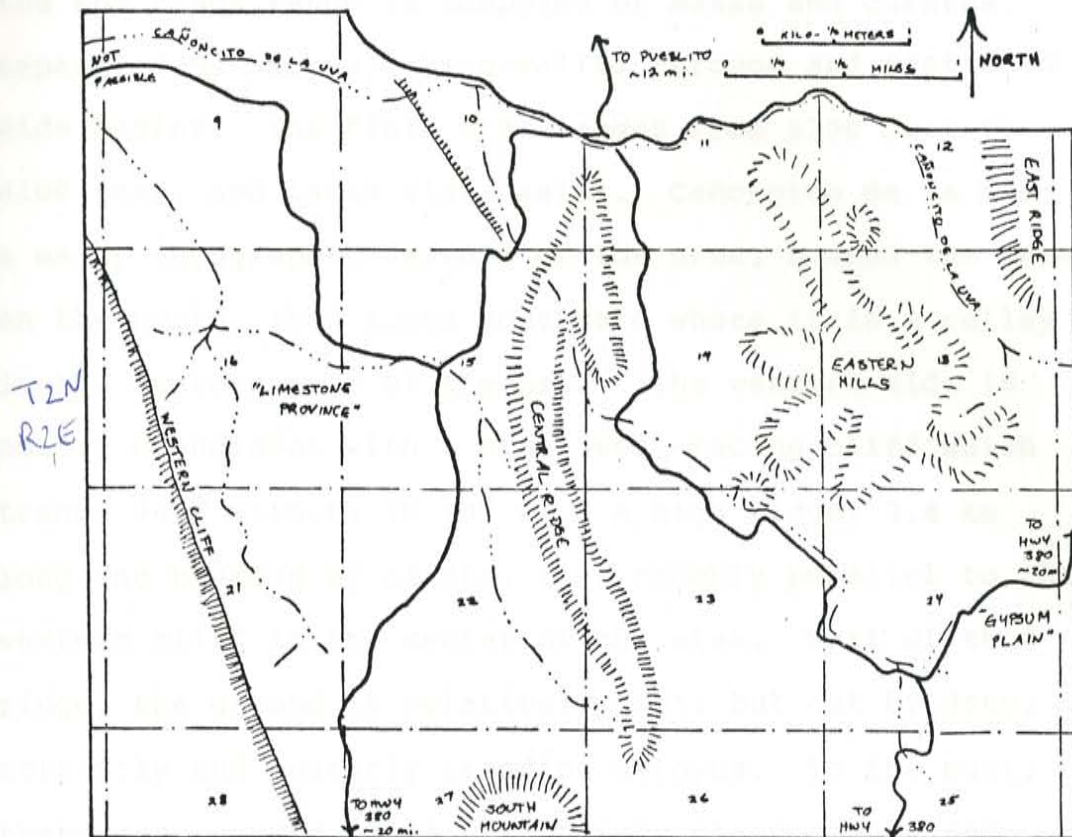


FIGURE 1: Location map and physiographic features of the southern Canoncito de la Uva area.

the Los Piños range is composed of mesas and cuestas, separated by narrow, steep-walled arroyos and scattered wide basins. The field area ranges from 5300 feet to 6100 feet, and lacks wide basins. Cañoncito de la Uva, a major topographic feature of the area, bounds the area on the north, then turns southward where it is a valley in the eastern part of the area. The western side is nearly coincident with a high, west-facing cliff which trends 340° azimuth (N 20° W). A high ridge, 3.4 km long and bounded by cliffs, lies roughly parallel to the western cliff in the center of the area. West of this ridge, the ground is relatively flat, but cut by deep, northerly and westerly trending arroyos. To the east, there are rounded hills with fairly steep slopes and mesa-like upper surfaces. The area is accessible by reasonably well-maintained Bureau of Land Management roads from Pueblito, a small community about 6.5 km (4 miles) north of Socorro.

Field Methods

Field investigation of the Cañoncito de la Uva area was conducted from spring 1985 to fall 1986. United States Geologic Survey 1:24,000 scale topographic maps were enlarged to 1:10,000 scale to provide a base for geologic mapping. Locations were determined by topographic features, triangulation, and pacing distances. Attitudes of outcrops and structures were

determined with a Brunton transit and a Silva Ranger type-C. Although the Ranger is not quite as accurate as the Brunton ($\pm 1^\circ$ vs. $\pm 0.5^\circ$), it is a lighter-weight, virtually unbreakable, more versatile tool. Attitudes of bedding and structure were recorded in azimuth readings. Field measurements were recorded in metric units. Stratigraphic sections were measured with a 1.5 meter jacob staff. Outcrops were described with the aid of a 10 power hand lens, millimeter scale, and GSA color chart. Samples of competent units were collected for thin section analysis of grain type, cement, and texture.

Major structures in the area are usually easily recognizable in the field: discordant bedding attitudes, offset, missing or repeated stratigraphic intervals, and zones of broken or incoherent strata are indicative. Some formations (notably the Abo Formation, and to some degree the Bursum Formation) conceal structures, especially faulting. Recognition of faults in these areas was based on more subtle expressions of the previously listed features, topography, and lineations observable on air photographs.

Previous Work

The first geologic map of the area was published at 1:407,430 scale by Darton in 1922. He mapped the formations broadly, divided into Magdalena Group

(Pennsylvanian), Abo Sandstone (Permian), and Chupadera Formation (Permian). In 1951, Wilpolt and Wanek did reconnaissance fieldwork in central Socorro County, however they added little to the work of Darton (1922) for T 2 S, R 2 E. Kottowski and Stewart (1970) described a section of the Bursum Formation in section 8 (T 2 S, R 2 E) at the northwest corner of this study area. Hunt (1983) described plant fossils in the Abo Formation collected in this field area. Maulsby (1981) mapped section 21, 28, and to the south and west at 1:12,000; my map is not completely consistent with Maulsby's map. Colpitts (1986) prepared a geologic map and cross sections immediately north of the area.

Works discussing regional geology important to this report include Stark and Dapples' (1946) paper on the Los Pinos Mountains, Seager and others (1983, 1986) on uplifts and basins in southern New Mexico, and several papers by Chapin and others (1978, 1979, 1981) discussing the Rio Grande rift.

Acknowledgements

I wish to express appreciation for all those who have helped me with this field work and report. First, my advisor, Clay T. Smith, for accepting me and encouraging me; Frank Kottowski and the New Mexico Bureau of Mines and Mineral Resources, for inspiration, a generous field grant, and occasional transportation;

David B. Johnson, for help with identification of stratigraphic units, discussion of paleoenvironments, and use of laboratory and personal equipment; and Charles E. Chapin for field days and intriguing discussions on structural geology. New Mexico Geological Society also provided field grant funds.

More than anyone, I wish to thank my friends here at New Mexico Tech, and the Institute generally, for continued, unyielding support: of ideas, of emotions, of laboratory equipment, of computerized editing and printing, and coffee.

STRATIGRAPHY

The stratigraphic units in this area are Pennsylvanian and Permian, marine and non-marine, carbonates, clastics, and evaporites. The works of Thompson (1942) and Rejas (1965) have been used to identify Pennsylvanian units. Thompson (1942) named and described units exposed in the Sierra Oscura, and divided the rocks into formations at lithologic contacts. Fusulinids (Triticites, Dunbarinella, Pseudostaffella(?)) found in Council Spring Limestone through Moya Formation are of Missourian and Virgilian age (Fig. 2). Rejas (1965) compared units present near Socorro to the lithologies, ages, and stratigraphic sequences described by Thompson (1942), and applied Thompson's names to lithologic units present in the Cerros de Amado area, central Socorro County. This paper follows Rejas' (1965) example, and applies Thompson's (1942) names to lithologic units exposed in the Cañoncito de la Uva area.

The oldest recognized unit, the Council Spring Limestone (Pennsylvanian), occurs in a small outcrop adjacent to a fault in the central part of the map area. Burrego Formation, Story Formation, Del Cuerto Formation, and Moya Formation crop out above the Council Spring. A complete section of Pennsylvanian and Permian strata is not available in this field area. In the southwestern part of

FIGURE 2: THE PENNSYLVANIAN SYSTEM IN CENTRAL AND SOUTHERN NEW MEXICO

SERIES	GROUP	FORMATIONS AND MEMBERS
Virgil	Fresnal	Bruton formation
		Moya formation
	Keller	Del Cuerto formation
Missouri	Hansonburg	Story formation
		Burrego formation
	Veredas	Council Spring limestone
		Adobe formation
		Coane formation
Des Moines	Bolander	
	Armendaris	Garcia formation
		Whiskey Canyon limestone
		Elephant Butte formation
		Warmington limestone member
Derry	Mud Springs	Cuchilio Negro formation
		Hot Springs formation
	Green Canyon	Apodaca formation
		Arrey formation

From Thompson, 1942, Table II, p.27

the field area, Moya Formation limestone, Bursum Formation clastics and limestones, and Abo Formation siltstones are exposed without major structural breaks above Burrego through Del Cuerto Formations. In the northeast part of the area, there is continuous exposure from Bursum through Abo, into sandstone of the Permian Yeso Formation.

Description of Units

COUNCIL SPRING LIMESTONE

The Council Spring Limestone is a 5.5 meter thick sequence of thin to irregularly bedded crinoidal wackestone and carbonate mudstone of Missourian age in the type area, the northern Sierra Oscura (Thompson, 1942). In Rejas' (1965) study area, 6.1 meters of Council Spring was measured. The base of the unit is not exposed in the Cañoncito de la Uva area, where it has a minimum thickness of 2 meters.

BURREGO FORMATION

Thompson (1942) applied the name Burrego Formation to 9.7 meters of grey, massive, nodular, Missourian age limestone in the Sierra Oscura. Near Loma de las Cañas, the Burrego exhibits differences in thickness and lithology over short distances. Rejas (1965) noted a marked increase in the thickness and clastic content toward the northeast

within his field area, and reported 26 meters of clastic sediments: greenish grey shales and siltstones, quartzitic arkose, and minor carbonate mudstone. Mauslby (1981) measured 102.4 meters of light olive-brown shales and other lithologies in an incomplete section. Bauch (1982) measured 60 meters, and reported that no limestones are present in the Burrego Formation in his area. Investigation of his field site revealed a few thin crinoidal grainstones within the Burrego Formation near his measured section.

Two incomplete sections of Burrego Formation are present in the Cañoncito de la Uva area. A significant portion of the top is missing in the west face of the central ridge. The base of the section is not exposed in the western cliff, where 69.4 meters (plate 7) were measured. The predominant lithology is calcareous siltstone, colored various pale gradations from olive to brown to grey. Some parts of the siltstone are micaceous; some are strongly to poorly fissile. Arkose, lithic sandstone, micaceous sandstone, packstone, and wackestone are interbedded with siltstone on a centimeter to five meter scale throughout the section. Thicker sandstone sequences display crossbed sets and convolute bedding. All sandstone beds have calcareous cement. The limestones are thin bedded and contain abundant marine fossil debris.

Low-angle tangential crossbed sets are common in the sandstones. These are arranged into medium and large (10 cm to 3 m thick) tabular and wedge-shaped sets. The dip direction of the crossbeds is roughly uniform throughout the section. Ripple marks of low amplitude (~ 1 cm) are present on some surfaces. Intervals of convolute stratification up to one meter thick are present within thick sandstone intervals.

STORY FORMATION

Thompson named 17.5 meters of Missourian strata the Story Formation. The lower 6 meters are shales and sandstones. The upper 11.5 meters are fossiliferous limestones. Rejas (1965) recognized two members of the formation, reporting 7 meters of arkose and shales in the lower member, and 4.9 meters of fossiliferous limestone in the upper member. Maulsby (1981) measured 9.5 meters of clastics in the lower member, and 6.8 meters of fossiliferous limestone in the upper member. In the Cañoncito de la Uva field area, lower clastic beds have been mapped as Burrego Formation, because Story clastics are not readily distinguishable from clastics of the Burrego in this area.

The boundaries of the limestone member are marked as the contacts on plate 1. The Story is best exposed along the western cliff and in arroyos east of there. Six meters of limestone are present at the site of plate 8. The formation is a cliff former, composed of medium to light grey, stylolitic, fossiliferous wackestones, packstones and grainstones. Abraded fossil debris of small size (less than 3 mm), is the most common organic component. Thin beds of crinoid grainstone are also present. Intraclasts up to several centimeters are present.

DEL CUERTO FORMATION

Thompson (1942) described 24.7 meters of Virgilian nodular limestone, arkose, and shales as the Del Cuerto Formation. Rejas (1965) recognized three members of the Del Cuerto Formation: the lower 5 meters of shale and arkose; the middle 6.1 meters, crinoidal grainstones; and the top 6.4 meters, sandy micrite and arkose. Maulsby (1981) found the lithology and thickness to vary from east to west within his study area. The Del Cuerto there is from 6.2 meters to 11.8 meters of carbonate mudstone, wackestone, and packstone. Bauch (1982) found 27.2 meters of fossil-poor carbonate mudstone and thin-bedded sandstones.

In the Cañoncito de la Uva study area, 7.5 meters of poorly exposed strata have been measured (plate 8). Much of the Del Cuerto Formation is covered throughout this study area. Various pink to dark red clayey soils cover the slopes. Medium beds of greyish red, arkosic limestone are the usual exposures. Friable, dark brownish red, laminated and trough-cross-laminated lithic sandstone outcrops are present locally. Thin, nodular, red-weathering limestone beds also occur. The base of the Del Cuerto Formation appears to be conformable over the Story Formation.

MOYA FORMATION

Thompson (1942) described 15.5 meters of fossiliferous Virgilian limestone as the Moya Formation in the Sierra Oscura. Rejas recognized two members: lower 11.8 meters of carbonate mudstone, and upper 11.6 meters of various lithologies unconformably overlying the lower mudstone. Beds of the upper member are carbonate mudstone, shales, and arkose. Maulsby (1981) measured 26.8 meters of Moya, in two members: carbonate mudstone, overlain by wackestones and less common packstones. Bauch (1982) found 42.8 meters of Moya, the lower 2 meters cherty and fossiliferous, but otherwise composed of unremarkable medium-bedded carbonate mudstone. The maximum thickness of Moya measured in the Cañoncito de la Uva area is 33.6

meters, however this is not a complete section.

The Moya Formation of the Cañoncito de la Uva area is predominantly fossiliferous limestone in apparent conformity with the underlying Del Cuerto Formation (Plate 8). However, sections of the Moya Formation from one place to another consist of significantly different sequences of strata (compare plates 9 and 10). Basal brachiopod or crinoid wackestone is present in most areas. This basal unit is commonly overlain by crinoid grainstone, stylolitic, fossil-debris packstones and wackestones, oolitic grainstones, and minor fine-grained, terrigenous clastic beds. Upper beds commonly have wavy surfaces and abundant distinct and indistinct intraclastic zones (Fig. 3). Grain-counts of the limestones show crinoids to be most abundant (Table 1, appendix). Low angle thick sets of crossbedded crinoid grainstones are present in two sections (Fig. 4, Plate 8, 9). Stylolitic and nodular beds are more micrite-rich, and have various types of abraded fossil fragments (fig. 5).

A few hundred meters to the southeast of a typical stratigraphic section (Plate 9), the thick limestone interval in the middle of the Moya is not present (Plate 10). In this exposure the basal wackestone is overlain by an 18.5 meter section of clastic rocks; much of this is convolute-bedded arkose (Fig. 6). It has calcareous



FIGURE 3: Intraclast breccia in Moya Formation.



FIGURE 4: Crossbedded crinoidal grainstones in Moya Formation.



FIGURE 5: Stylolite detail in Moya Formation.



FIGURE 6: Convolute sandstone bed in Moya Formation.

cement. Limestone beds capping this section are identical to beds capping nearby limestone sections.

BURSUM FORMATION

Wilpolt and others (1946) originally described the Bursum Formation, determined it to be of Wolfcampian age, but indicated no type section for the red and green shale, arkose, and limestone beds. The base was described as composed of reworked limestone clasts from the underlying uppermost Madera Formation (now recognized as Moya) (Wilpolt and others, 1946). Rejas (1965) reported 61 meters of grey-brown arkose, pebbly conglomerate, red calcareous shale, sandy intraclast beds and recrystallized carbonate mudstone. Maulsby measured 76.7 meters of Bursum, noting that the basal contact is unconformable with underlying limestones. Alteras (M. S., in progress) measured five sections of the Bursum, two of which are within the boundaries of this field area. His Del Cuerto section, included in this report (Plate 11), is 46 meters thick.

In the Cañoncito de la Uva area, the base of the Bursum Formation is locally marked by different rock types above and below it. In all cases the contact has clastic sediments deposited over Moya Formation limestone. In some places the top of the Moya has channels eroded into it, and these are filled with creamy white, medium-grained, well

indurated sandstone. In other places a veneer of limestone conglomerate (composed of clasts of Moya lithology) covers the top of the Moya. Red or grey siltstone is deposited on Moya in some locations.

The Bursum Formation is exposed as shaly slopes with small resistant ledges in the Cañoncito de la Uva area. Alteras (M.S., in progress) subdivided, the Bursum into three zones: a lower clastic sequence composed of medium grey, medium reddish grey and purplish grey calcareous shales, claystones and siltstones; a middle carbonate interval containing thin to thick bedded, silty, nodular bedded, cherty and/or fossiliferous limestone, shale beds, and minor amounts of sandstone beds; and an upper mixed zone containing trough-crossbedded sandstone, grey shales, and arkosic limestones; with fewer purplish and reddish shale beds. Many beds, especially those composed of crossbedded sandstone or pebble conglomerate, are discontinuous over distances of less than half a kilometer.

ABO FORMATION

Needham and Bates (1943) defined a type locality and type section for the Abo Formation, originally described by Lee (1909). Needham and Bates (1943) measured 274 meters of red shale, sandstone, arkose, and conglomerate, containing halite casts, mudcracks, extensive crossbedding,



FIGURE 7: Bursum Formation exposures in s. 14.

wave and current ripplemarks, and animal and plant fossils. These features indicate a continental origin for the formation. Fossils collected by Hunt (1983) from the Cañoncito de la Uva exposures of Abo are of Wolfcampian age. The thickness of the Abo varies greatly from place to place (Kottlowski, 1963)

The Abo Formation is exposed throughout the eastern half of the Cañoncito de la Uva area (Fig. 8). A complete section is difficult to recognize because the siltstones readily conceal faulting. It appears to be ~200 meters thick. Cliff-forming outcrops are composed of reddish brown sandstone and siltstone. Poorly exposed and covered intervals are made up of reddish brown mudstone and shales. Coarse siltstone and fine to medium grained sandstone beds are variously arranged in thinly laminated sets, wedge-shaped crossbedded sets, and cross-laminated sets. Ripple marks of low amplitude, mudcracks, and plant impressions occur on some bedding surfaces. Sandstone outcrops are subordinate to mudstone lithologies by a one to four margin, but increase in thickness and frequency from the middle to the top of the formation. Grain-counts show the predominant mineralogy to be quartz and clay (Table 1).



FIGURE 8: Westward from east ridge: Abo exposures in middleground, Bursum at the base of the slope on both sides of the wash.

YESO FORMATION

The Yeso Formation is composed of four members in central New Mexico: the Meseta Blanca, Torres, Cañas, and Joyita (Jicha and Lochman-Balk, 1958). The Meseta Blanca Member originally was measured and described as part of the Abo Formation (in Needham and Bates, 1943), but is correlated with the Meseta Blanca Sandstone (of Wood and Northrup, 1946) by Read (in Bates and others, 1946). Needham and Bates (1943) described three members in their remeasuring of the designated type section of the Yeso Formation described by Lee (Lee and Girty, 1909). Their lower clastic zone (an interbedded sequence of limestone, siltstone, gypsum and shale) was named the Torres Member by Wilpolt and others (1946). Needham and Bates (1943) named a thick gypsum bed the Cañas Member, and nonresistant, crossbedded sandstones the Joyita Member. Flower (in Kottlowski and others, 1956) dated the fauna as Leonardian age. Only the lower two members are exposed in this field area.

MESETA BLANCA MEMBER: The Meseta Blanca Member crops out along the eastern side of the map area. In the north and south, it is incomplete, broken by complex faulting and folding. The beds exposed in the east halves of sections 12 and 13 appear to be continuous; however the top is absent, and bedding-plane faults are present east of that locality, on the east-facing hillside just out of the map

area. these faults project into the section through the hill. Colpitts (1986) measured 89.5 meters of strata 3/4 km north of the northwest corner of the Cañoncito de la Uva area (secs. 4, 5). This is the nearest reliably complete section to the Cañoncito de la Uva area.

In the map area, the Meseta Blanca Member is conformable over the Abo Formation. The contact is placed at the base of a thick set of (commonly) pale yellow colored, planar sandstone laminations that is directly or closely below horizons containing impressions of halite crystals. These criteria occur at slightly different levels in the strata from one exposure to another. Salt casts are not present (or visible) near the boundary at every exposure, and the sandstone unit proved to be a more reliable, traceable mapping boundary. The Meseta Blanca is composed of interbedded, tabular-shaped sets of sandstone and siltstone laminations. The sandstone is pale yellowish grey to pale red to dark reddish brown, is thick bedded to laminated, and displays symmetric and asymmetric ripple marks, convolute laminations and salt casts. Color of beds commonly changes along strike (Fig. 9), and therefore cannot be used as a reliable marker for stratigraphic correlation or structural interpretations. Siltstones are similarly colored, contain mica and carbonaceous debris, and have more common convolute laminations and salt casts.



FIGURE 9: Discoloration of beds in Meseta Blanca Member, view northeast from Baca well.

The upper contact with the Torres Member is exposed near the thrust fault in the southeast part of the map area (secs. 13, 24).

TORRES MEMBER: The Torres Member is incomplete in the Cañoncito de la Uva field area. The base, deposited upon red and grey Meseta Blanca Member, is a carbonate mudstone bed about one meter thick. Red sandstones appear to be intercalated between grey limestone beds at the base, but this relationship may be structural in origin. The sandstones were mapped as Meseta Blanca. Upward through the section, the unit is interrupted by faults and folding, and a continuous section is not available within or nearby the field area. The upper beds, exposed in sections 24 and 25, are poorly exposed, pale red siltstone, sandy siltstone, pale grey gypsum and gypsiferous siltstone beds. Outcrops rarely exhibit bedding, and in those that do, the attitudes are chaotic and suspect: probably a function of dissolution and/or viscous disruption, and not indicative of structural features in the area.

DEPOSITIONAL HISTORY

Deposition of sediments in the Cañoncito de la Uva area occurred first in marine, then in nonmarine, and lastly in marine, environments. The first transition is represented by probable deltaic facies occurring between marine limestones and fluviatile mudstones. The Pennsylvanian sediments are characterized by alternations of siliciclastic and carbonate sedimentation. The character of this sedimentation package reflects worldwide changes in sea level, probably caused by late Paleozoic glaciation. However, coarse arkosic sands, large volumes of limestone rubble, and rapid lateral changes in thickness of beds and units suggest this variability may also be due to local tectonic activity at the time of deposition. Local source areas are implied by angular, feldspar-rich, siliciclastic debris; and lateral thinning and thickening of clastic units suggest local basin subsidence occurred during deposition of those sediments.

The oldest sediments of the area are marine. Council Spring Limestone is marine, but not adequately exposed to interpret conditions of deposition. The overlying Burrego Formation is composed of poorly-sorted calcareous siltstones, sandstones with uniform cross-bed dip direction, and thin lime grainstones, all of which indicate marine deposition. Transition from the lower fine grained material to better-sorted coarser-grained sediment in the

upper part of the unit indicates a shallowing of the marine environment, bringing the sea floor closer to wave base. This shallowing could have been caused by eustatic sea-level lowering, uplift of the sea-floor, or progradation of the shoreface into the basin, or combinations of these events. Compaction of the sediments, probably due to dewatering of silt shales, could have caused convolution of intervals of sandstone sequences.

The Story Formation is a relatively siliciclastic-free limestone, with abundant abraded fossils. Shallow marine shelf is the probable depositional environment for these fossiliferous limestones. Grainstone deposits show the basin floor at the time of sedimentation was above wave base, allowing wave-swash to winnow out finer sedimentary particles. Micrite-rich beds were deposited in quieter water areas, probably where wave-swash was dampened by aggradation of carbonate-producing organisms to sea level, or perhaps deepening of the basin to below wave base. I favor an aggradational dampening interpretation for the lime mudstones, because deepening of the basin could lead to a dieout of carbonate organisms, many of which are light-dependent. However, lack of clastics represents a time during which the clastics become trapped at river outlets and are not deposited in the basin, often caused by sea level rising. These two processes may not be contradictory, and perhaps are the best evidence of eustatic rise of sea level. Deposition of significant

thicknesses of carbonate rock must be accompanied by a relative rise in sea level, for the organisms responsible for deposition can only aggrade to the water surface.

Minor amounts of fossils in the clastics of the Del Cuerto Formation show it was deposited in a marine environment. Lack of carbonate deposition during this time may be due to inundation of the basin by a prograding delta lobe, increasing the turbidity of the water beyond the tolerance of filter-feeding organisms, or by deepening of the basin, resulting in the death of light-dependent carbonate organisms. Again, deepening may be tectonic or eustatic in origin.

Basal Moya Formation limestone over Del Cuerto Formation represents marine conditions. Cross-bedded Moya grainstones and oolites suggest an aggradational, wave-washed shoal was present. The adjacent thick sandstone sequence, floored by intraclastic lag upon limestone, and capped by marine limestone, may be a bypass-channel deposit, where clastic debris from uplifted terrigenous areas were transported to the floor of the marine basin.

The Bursum Formation is composed mostly of mudstones. Reworking of underlying limestones, and fluvial features within sandstones show regression of the sea. Marine limestones are present within the section, although subordinate to the clastic beds. Alteras (M.S., in progress) interprets

the Bursum as a sequence of delta lobes. My observations of pre-Bursum marine limestones, post-Bursum fluviatile siltstones, and changes in facies thicknesses and sequence from one area to another, support his interpretation. Again, some of these features may be due to large eustatic variations in sea level, especially the limestone in the middle part of the section. Coarse clastics in the section show local source areas for this sediment, perhaps a function of syndepositional tectonism. Some of the mudstones could have been deposited on a fluviatile coastal plain, where subsidence kept lowering base level, allowing aggradation of a significant thickness of sediment. Regardless, continued influx of clastic sediments resulted in delta and shoreline progradation. Eventually the area was entirely overrun by terrestrial sediments of the Abo Formation.

The river sedimentation continued in a subsiding, low relief area, indicated by the high proportion of mudstones in the lower part of the Abo Formation. Coarser channel deposits are present higher in this formation. The Meseta Blanca Member marks the return of marine conditions, but the basin may have been shallow and somewhat restricted. Salt casts in the lower part of the member show salt water did evaporate. Symmetric ripple marks on bedding surfaces indicate shallow water, where wave oscillation shaped the basin floor. Tabular-shaped sets of low-angle crossbeds were deposited by waves on a shallow marine shelf.

Eventually there were more normal marine conditions, when the limestones of the lower Torres Member were deposited. However, restricted conditions returned to deposit gypsum of the upper beds of the Torres Member. These shallow marine sediments represent a period of quiescence and regional subsidence, when tectonic uplift of the ancestral Rocky Mountains had ceased.

STRUCTURAL GEOLOGY

Cañoncito de la Uva is located on the east side of the Rio Grande rift. Some extensional faulting affects the rocks. Additionally, compressional tectonics previous to rift opening, which is also exposed in ranges to the north and south of the area, is evident in this area.

Exposures of faults are generally recognized by omission or repetitions of a stratigraphic sequence. Offset beds, missing parts of units (or entire units), and repeated beds are commonly accompanied by abrupt changes in bedding attitudes, breccia zones, resistant breccia "dikes", anastomosing fracture patterns (on a cm spacing), and slickensided surfaces (Figs. 10-15). In some areas these accompanying features are present, but faulting is not obvious. Comparison of these areas to aerial photographs of the region show lineaments present, and it is assumed faults are present. Fold axes are not well exposed, and stereographic construction was employed to discover axial trends and plunges.



FIGURE 10: Drag folds on fault, s. 9, view northeast, Bursum Fm.

FIGURES 11-15: Fractures along faults



11: Abo Formation, foliation imparted, compass points north, s. 23.



12: Torres Member, breccia dike in channel, s. 13



13: Abo Formation, intersecting breccia dikes, s. 9.



FIGURE 14: Abo Formation, cataclastic texture, compass points north, s. 24.



15: Moya Formation, right-stepping extensional fractures in s. 16.

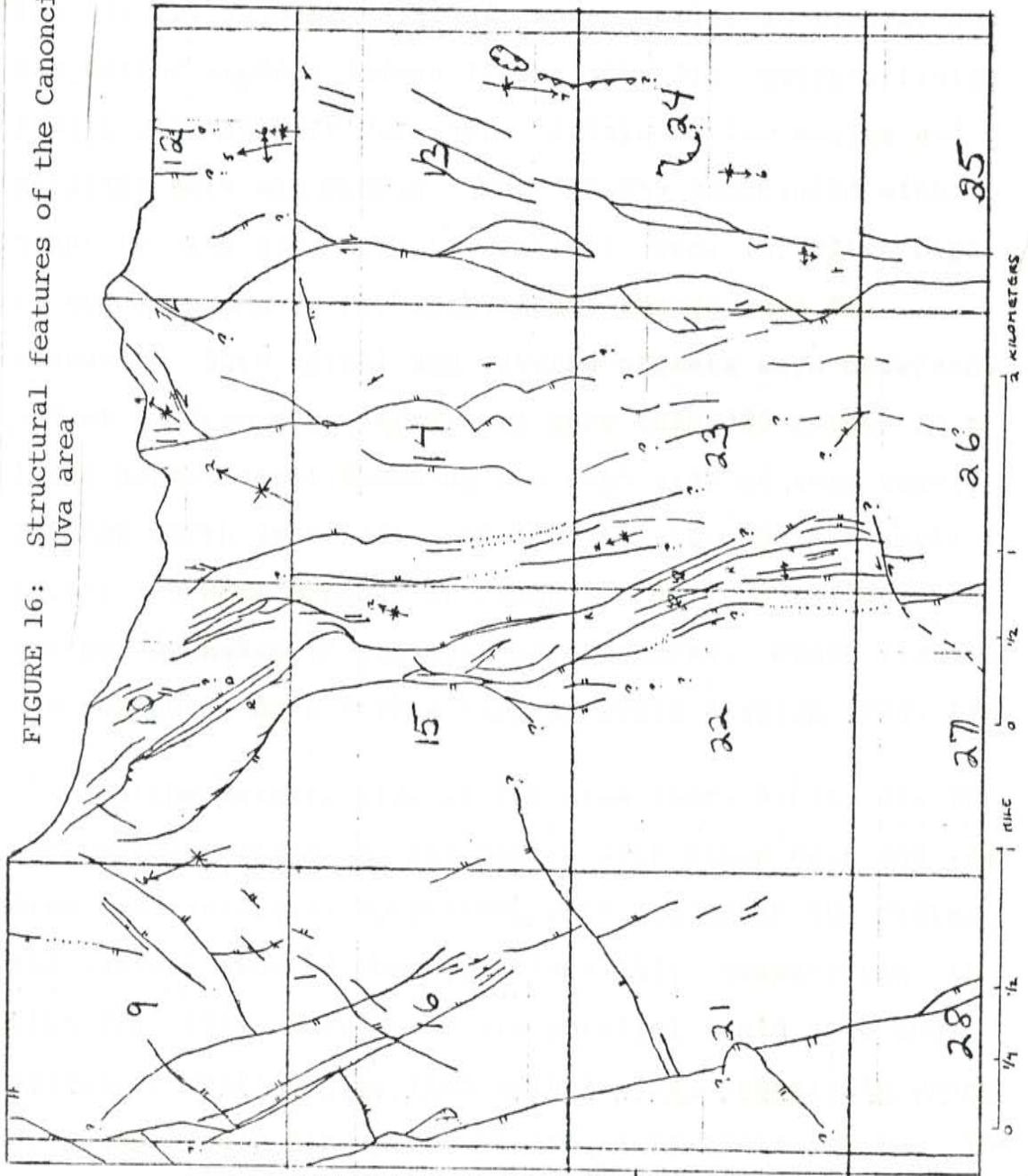
Description of Structures

FAULTS

Most major faults and many smaller faults strike close to north (Fig. 16). Smaller faults strike northeast, dip variously northwest or southeast, and appear downdropped to the southeast more commonly. Low-angle reverse faults are exposed within the Yeso Formation in the southeast corner of the map area, and in the Moya Formation in the central ridge. The following paragraphs amplify the description of these fault patterns. For clarity, location is described in terms of landform, with section(s) indicated parenthetically.

In the eastern side of the field area, fault planes are not well exposed (sec. 11-14, 23-26). Faults are anastomosing ("braided") at small angles to the overall trend (class I in Table 2). Breccia within fault zones shows a marked fabric in some places. A north-northwest-trending zone in Abo Formation (Fig. 11) is spanned by a left-stepping en-echelon pattern of fractures. Crude foliation is locally shown in more cataclastic zones (Fig. 14). These patterns are the result of clockwise (right-lateral) deformation. Most exhibit an apparent west-side-down offset from one to ten meters. Those with apparent east-side-down movement have lesser offset, in both normal and reverse directions. Where dips are unknown, they have been assumed vertical for structural

FIGURE 16: Structural features of the Canoncito de la Uva area



cross-sections and stereographic diagrams (Plates 2 to 6; Figs. 17, 18).

Faults* in the central part of the field area (secs. 10, 15, 22, 23, 26; Fig. 16) have similar attitudes, but are better exposed (class II in Table 2). North-striking faults are the most distinct; splays at low angles and parallel sets are common. Many faults associated with tight folding dip close to vertical (sec. 15, 22). Dips to the east and to the west occur, though more dip westward. Both normal and reverse offsets were observed. Offset is from a few meters to more than 200 meters on a large normal fault bounding the west side of this zone. Further north (sec. 10) west-dipping, low-angle reverse faults are well exposed in Cañoncito de la Uva. Some steepen downward in the outcrop exposures. Class I and II are contoured on a b-pole stereographic diagram (Fig. 17).

On the western side of the area (sec. 9, 16, 21, 28), northerly-striking, normal faults with steep east and west dips have attitudes consistent with faults in the center and eastern side of the map (class III; compare Fig. 18 with Fig. 17). There also are parallel fault sets and splays at small angles from main faults, especially where they apparently die out southward along their strike. The normal fault bounding the cliff on the west has at least 200 meters of offset (Fig. 19). Along this fault there are small fault-bounded blocks (pieces, really) deformed

FIGURE 17: STEREOGRAPH OF CLASS I AND II FAULTS

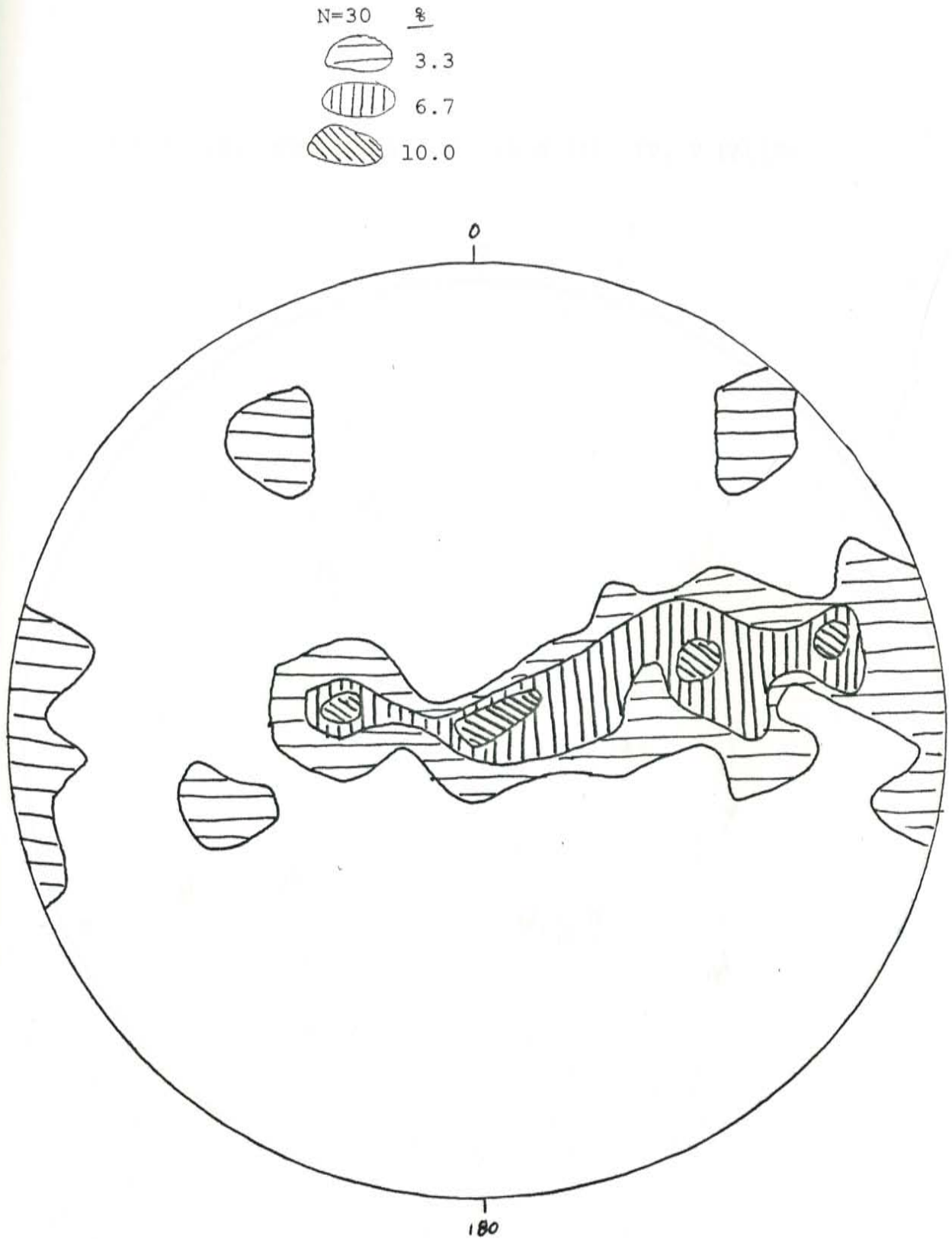


FIGURE 18: STEREOGRAPH OF CLASS III, IV, V FAULTS

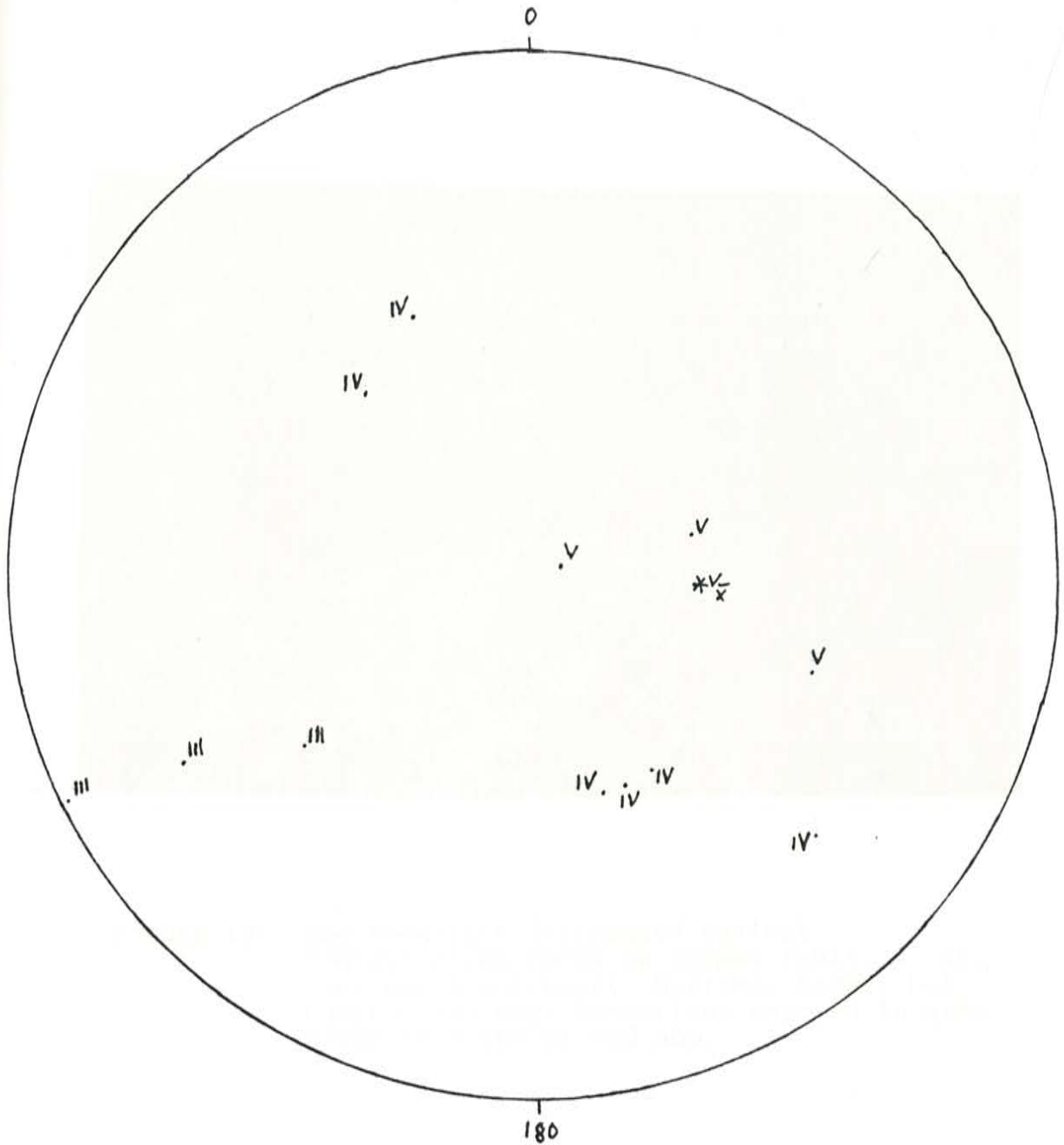




FIGURE 19: Abo Formation juxtaposed against Pennsylvanian rocks on normal fault, s. 20, view north-northwest; Burrego, Story, Del Cuerto, and Moya Formations exposed in grey slope to right of red Abo.

into northwest-plunging anticlines (see Plate I). The strata of these blocks is older than the rocks exposed to the west, and younger than rocks to the east of them.

Northeast striking faults are less common, have less stratigraphic offset, and are less extensive laterally than those in northerly trending sets (class IV). Northeast striking occur throughout the field area (Fig. 10 illustrates one), but are better exposed in the western half. In one case, dips toward the northwest and southeast are present on the same fault (sec. 9). Most have apparent displacement down to the southeast. In places these smaller faults apparently crosscut northerly ones. At the south end of the central ridge (sec. 26) the northeast-striking fault offsets nearly vertical normal faults. Northerly faults also appear offset in some exposures on the western side of section 9 and 16, but in section 9, a northeast-striking fault terminates against a north-northwest-striking fault.

Exposures of thrust faults are uncommon. In the central ridge (sec. 15), a low angle, subhorizontal fault truncates the bottom of west-dipping stylolites (Fig. 20). Slight curvature of the stylolites into the fault plane suggests movement was from the east. The fault plane is quite sharp, and does not contain gouge or breccia. In the southeast part of the map area (sec. 13, 24), some thrust relations in the Yeso Formation are present (class V).

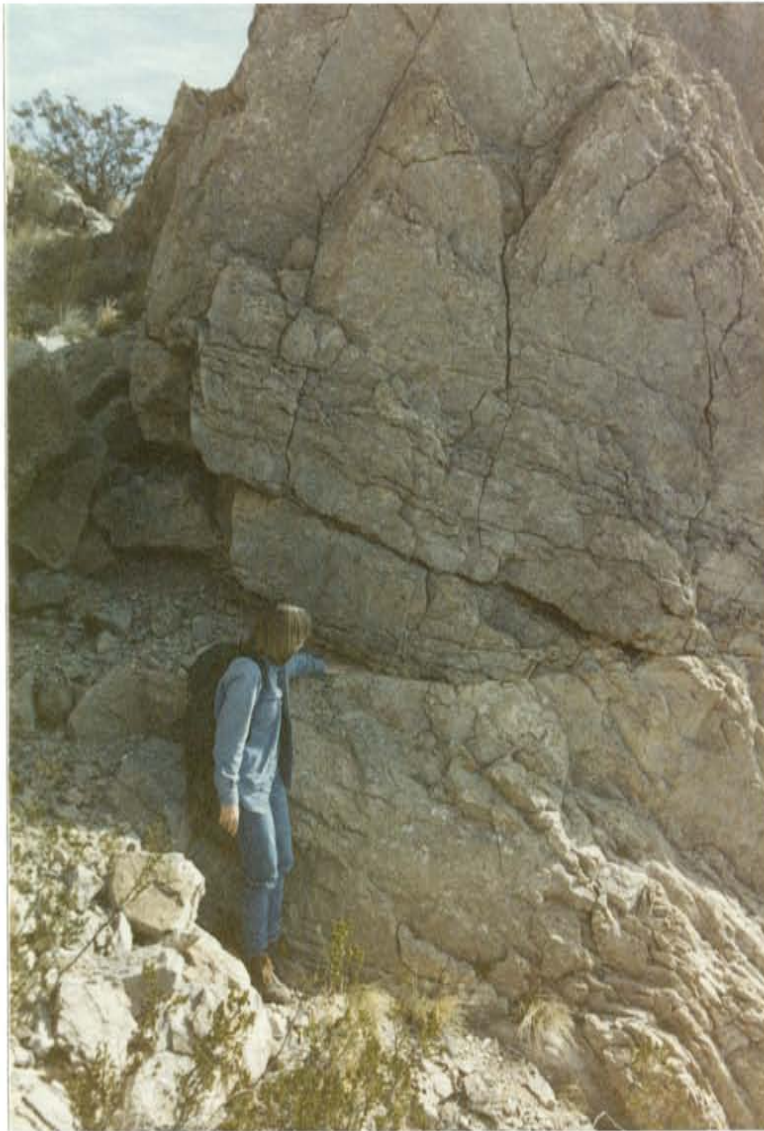


FIGURE 20: Small, low-angle reverse fault in central ridge.

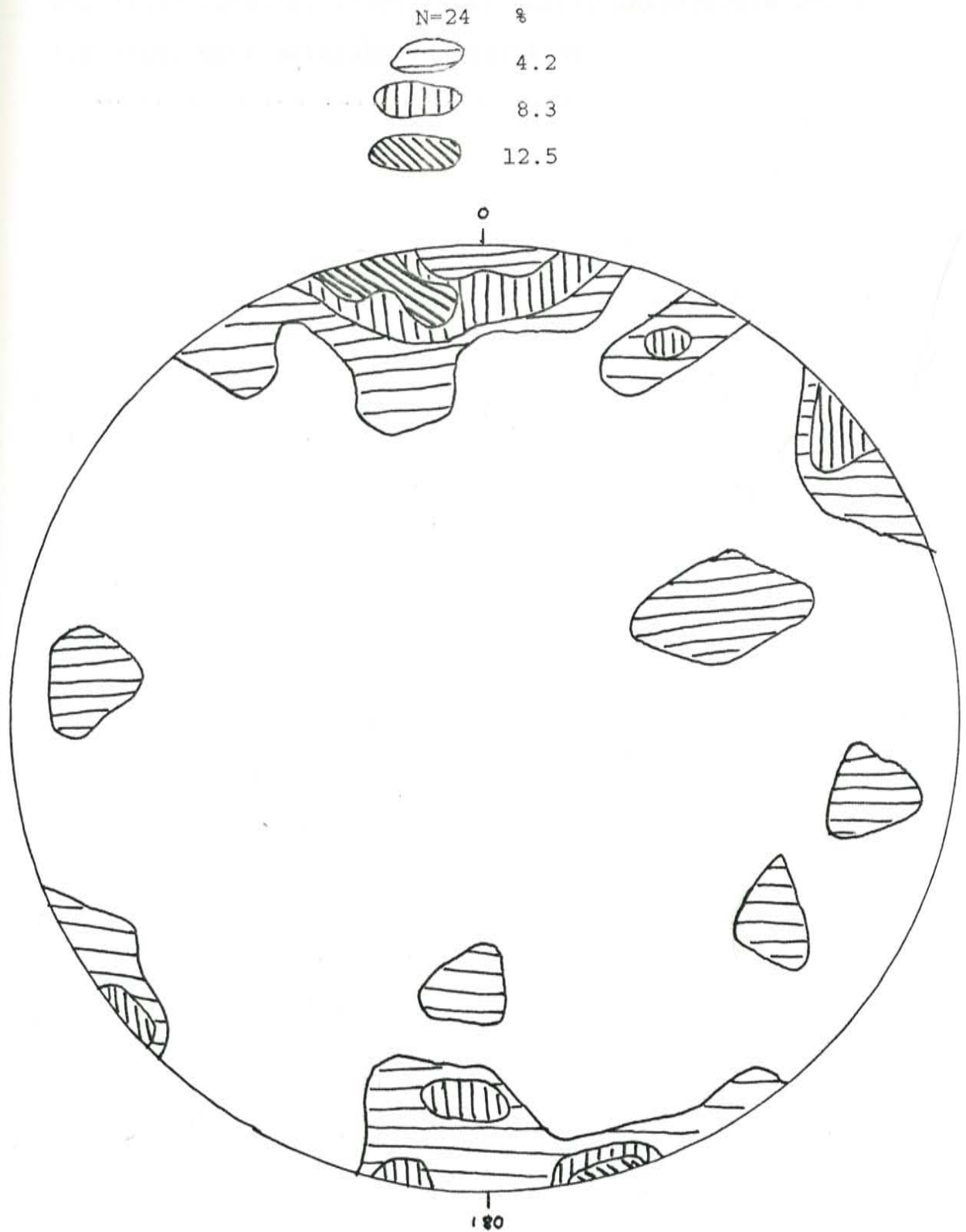
Outcrops are not good, and folding complicates recognition of fault outcrops and fault planes. The exposure trends northeast, and the average attitude of planes has a northerly strike, and a westerly dip of about 45° .

FOLDS

Most folds in the area have subhorizontal axes (Fig. 21, Table 3). The most prominent fold set in the area is located in the central ridge. Pennsylvanian strata form an isoclinal anticline, with the northeast limb overturned in the middle part of the ridge (sec. 22, 23). This fold trends 340° , and the axial plane dips west. Small-scale folds of similar trend occur on the north end in small fault blocks (SE 1/4 of sec. 10), and discontinuous open anticlinal segments occur from the east half of section 15, southward through the west half of section 23. Faults cut the segments, and fault planes do not appear to be folded.

Small open folds adjacent to faults are present in the eastern half of the map area. In most cases, the axes of folds trend less than 35° from the trend of the fault zone they occur near. A few (notably those in central sec. 15) have considerable axial plunge. These folds are not laterally extensive; they die out within a few hundred meters of the fault they occur near, and also are truncated by faults in some places. Along the eastern thrust fault (sec. 13, 24), an open anticline-syncline pair is present in the lower plate. These trend northeast and south,

FIGURE 21: FOLD AXES STEREOGRAPH



respectively, and plunge only slightly. Folding in the western part of the area is mostly long wavelength, low amplitude warping, which is virtually untraceable due to low dips, poor outcrops and faulting.

Regional and Comparative Structure

The Los Piños Mountains are composed of Precambrian supracrustal and intrusive rocks, nonconformable Pennsylvanian and Permian sedimentary rocks, and Quaternary volcanic rocks (Stark and Dapples, 1946). Stark and Dapples (1946) mapped west-dipping Paloma and Montosa faults in Precambrian and Paleozoic terrane. The structures originated in the Precambrian, but later reverse movements thrust Precambrian rocks over Paleozoic rocks along the faults. The faults are subparallel, decrease in throw southward from at least 1200 feet (360 m) to less than 100 feet (30 m), and are marked by silicified breccia, steepening of bedding attitudes (to vertical), and bedding slip movements. The Montosa has major, subparallel splays. Strata between the Montosa and Paloma faults are deformed into an overturned anticline (Stark and Dapples, 1946). Features similar to those associated with the Paloma and Montosa faults occur in the Cañoncito de la Uva area.

Smith (1983) describes folding south of Cañoncito de la Uva in the southern Los Piños. Crumpled zones and overturned eastward-verging anticlines in Pennsylvanian and Permian strata are exposed in and south of Arroyo del Tajo (sec. 18, T 3 S, R 2 E), south of Ojo de Amado in Arroyo de los Piños (sec. 27, T 2 S, R 1 E), southwest of Ojo de Amado (sec. 35, T 2 S, R 1 E), and in section 20 and 29

(T 4 S, R 2 E). Colpitts (1986) has mapped the Montosa fault in his field area. This structure strikes northeast, dips southeast, is anastomosing, and has 300 to 400 meters of throw. He interprets it as a right-lateral wrench fault on the basis of fold axes striking north-northeast ($\sim 50^\circ$ into the trend of the fault zone). Thrust relations of Paleozoic rocks over Triassic rocks, and small "horses" (Fig. 22; pods of rock completely bounded by two or more fault surfaces, which may consist entirely of inverted strata in thrust areas; Boyer and Elliott, 1982) are also present in his field area. Reconnaissance mapping southwest of the Cañoncito de la Uva area revealed a northeast-striking wrench fault with features suggestive of right-lateral movement. This fault, which I name the Del Curto fault, strikes southwestward through the Del Curto ranch headquarters, north of Loma de las Cañas, toward the folds exposed in Arroyo del Tajo, and northeastward toward the southern end of the central ridge in the Cañoncito de la Uva area. Dr. Charles Chapin and I followed the vertical structure (previously mapped by Maulsby, 1981, as a normal fault), and found slickensides in several directions (including horizontal, parallel to the ^{strike of the} fault plane) and small, tight, plunging folds (15° to 80° plunge toward 210° to 240°) along the fault. More northerly striking splays, with lesser offset, are also present. The offset on the Del Curto fault decreases northeastward along

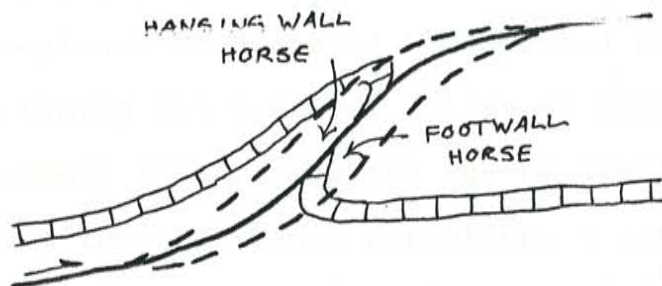


FIGURE 22: Cross section through incipient horses. New fractures (dashed) may cut horses from either footwall or hanging wall of major thrust surface. Strata of horse need not be overturned as this diagram shows. From Boyer and Elliott, 1982, figure 9, p. 1199.

strike, from a point one kilometer southwest of the headquarters (sec. 33) toward the Cañoncito de la Uva area (sec. 26).

Further southward, in the Cordilleran overthrust belt, extensive thrust plates with associated folds and imbricate thrust platelets (Fig. 23) were moved northeastward during the Piman phase of the Cordilleran orogeny (~75 Ma) (Drewes, 1982). In southwestern New Mexico, imbricate thrust faults in Paleozoic and Cretaceous formations may have splayed off of an underlying decollement. Outcrops in the Brockman Hills, Florida Mountains, Animas Gap, and Big and Little Hatchet Mountains suggest the presence of strike-slip-plus-thrust faults with oblique movement (Drewes, 1982).

Seager (1983), and Seager and others (1986) have identified regional compression accompanied by substantial crustal shortening and vertical uplift of Laramide age. Seager and others (1986) show the age by overlap and deformation of the Love Ranch Formation, a late Paleocene to Eocene conglomerate deposit. Their work in the southern Caballos has shown northwest trending basement blocks are bounded on the northeast by narrow deformed belts of reverse faults and strongly overturned folds (Fig. 24). Note the similarity of style to geologic cross sections F-F' and G-G' (Plate 4).

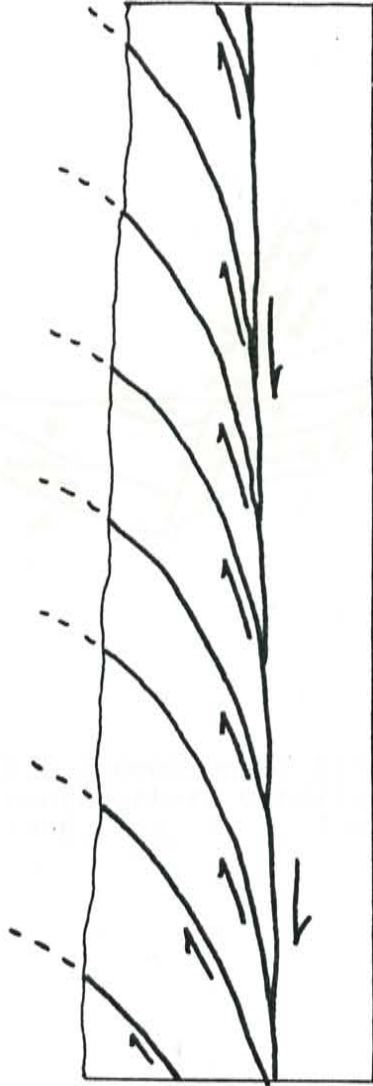


FIGURE 23: Cross section of imbricate thrust sheets, which merge asymptotically downward to a common basal sole thrust. From Boyer and Elliott, 1982, figure 11, p. 1199.

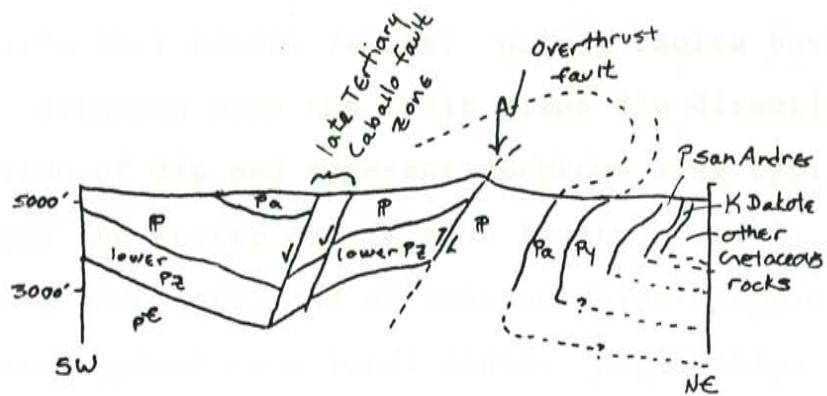


FIGURE 24: Cross section of Rio Grande uplift in the southeastern Caballo Mountains, from Seager, 1986, fig. 7, p. 128.

Hafner (1958) described zones with differential vertical uplift of basement rocks, and showed characteristic reverse faults which steepen at depth (Fig. 25). Harding (1985) documents reverse faults which steepen at depth as products of a transpressive wrench regime (Fig. 26). He calls these positive flower structures.

Harding (1985) provides a criterion for distinguishing wrench faults from normal faults: normal faults have consistent upthrown side and fault plane dip direction; the direction of dip and apparent upthrown side typically varies along the strike of a wrench fault. Curved, anastomosing (braided), and en echelon (side-stepping) patterns are typical on a local scale. Regionally, wrench faults can exhibit transpressive (compressional) or transtensional (divergent) zones (Fig. 27; Reading, 1980).

The suite of deformational styles which wrench regimes are subject to can identify the trend and displacement sense of wrench zones. Wilcox et al. (1973) modelled parallel, transpressional and transtensional wrench faults. They identified principle elements of wrench patterns: en echelon folds with axes at low angles to the wrench zone, conjugate strike-slip faults (a 10-30° set with the same sense of displacement, and a 70-90° set with opposite displacement), the main wrench zone, and normal faults and

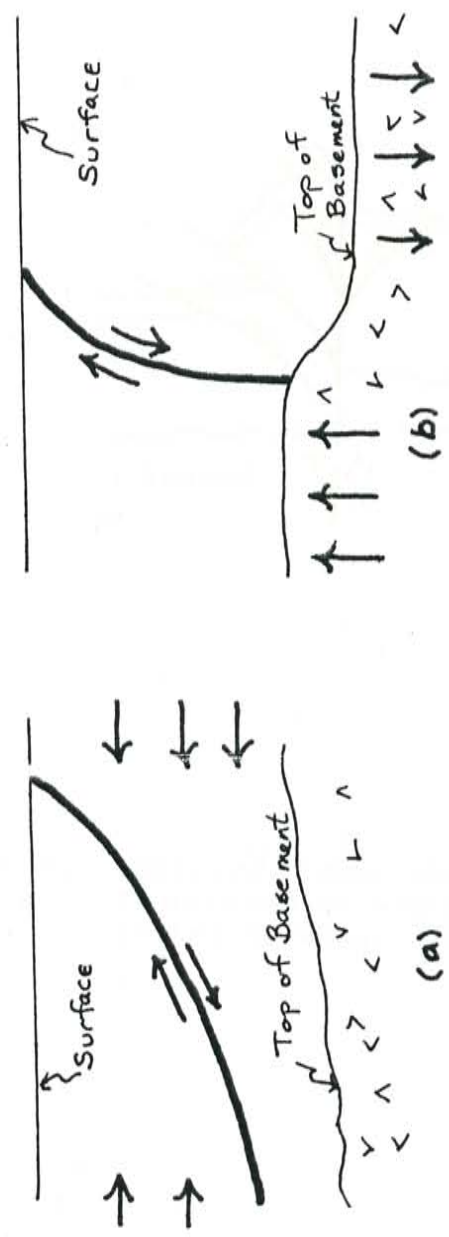


FIGURE 25: a) Overthrust due to compression
b) Upthrust due to differential vertical uplift
from Hafner, 1958, fig. 2, p. 2.

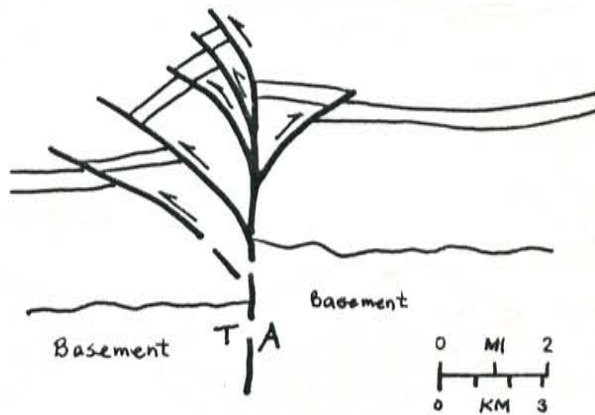
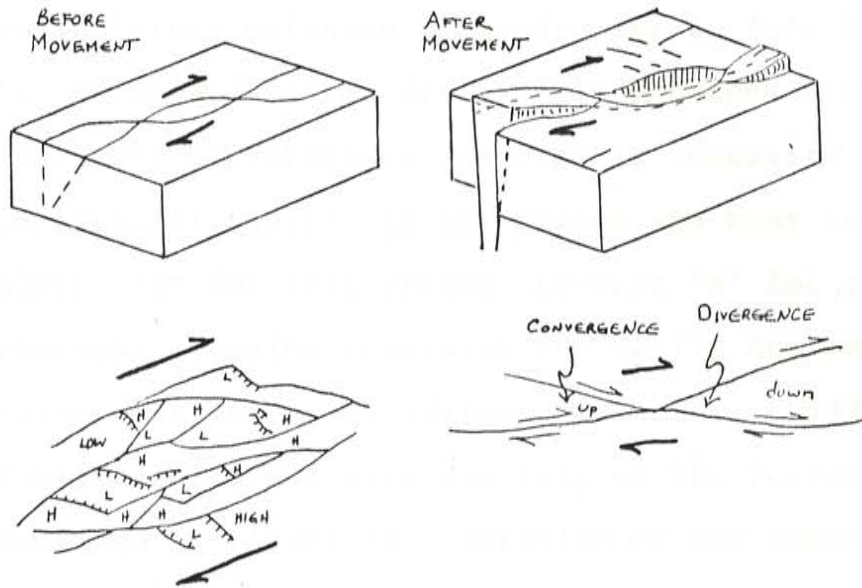
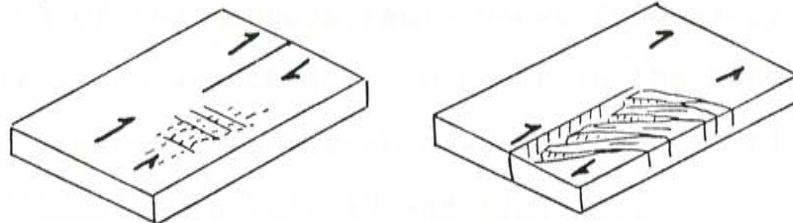


Figure 26: Positive flower structure produced in a transpressive wrench regime (after Harding, 1985, p. 593).

CURVED FAULT TRACE LEADS TO ANASTOMOZING PATTERNS



FAULT TERMINATIONS



EN ECHELON WRENCH FAULTS

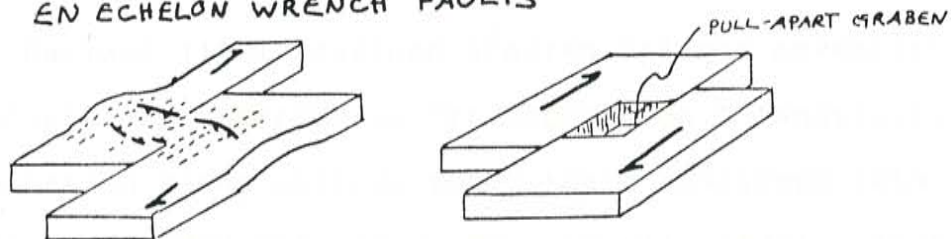


FIGURE 27: Types of strike-slip fault patterns, which produce subsided basins and uplifted blocks. From Reading, 1980, figure 3, p. 12.

tension joints oriented perpendicular to fold axes (Fig. 28). En echelon folds are greatly enhanced with even slight (2°) convergence. Antithetic (opposite displacement) faults can be rotated and bent into flat "s" shapes: "s" for left-wrench, reverse "s" for right-wrench movements. Tension fractures are easily destroyed as displacement increases (Wilcox, and others, 1973). The Cañoncito de la Uva area has many of the features which are summarized in figure 28. Rotation of the figure to bring the arrows indicating wrench movement parallel to the strike of the Montosa fault shows fold axes, reverse faults, and wrench zones present in the Cañoncito de la Uva area are consistent with a wrench-fault explanation. (Data is presented in Fig. 17 and Fig. 21.)

Harland (1971) defined sheared oblique movement in Caledonian Spitsbergen as "transpression." Penetrative deformation along oblique zones there developed into an upthrust-bounded welt (Fig. 29; Lowell, 1972). There are numerous examples of folds and thrusts along other oblique-slip faults (i. e. San Andreas: Dibblee, 1977; Moody, 1973; Sylvester and Smith, 1976; Alpine, New Zealand: Sporli, 1980; etc.).

Transtensional regimes develop pull-apart basins, named "rhomb grabens" by Freund (1982). These are bounded by normal and wrench faults, and receive sediment from

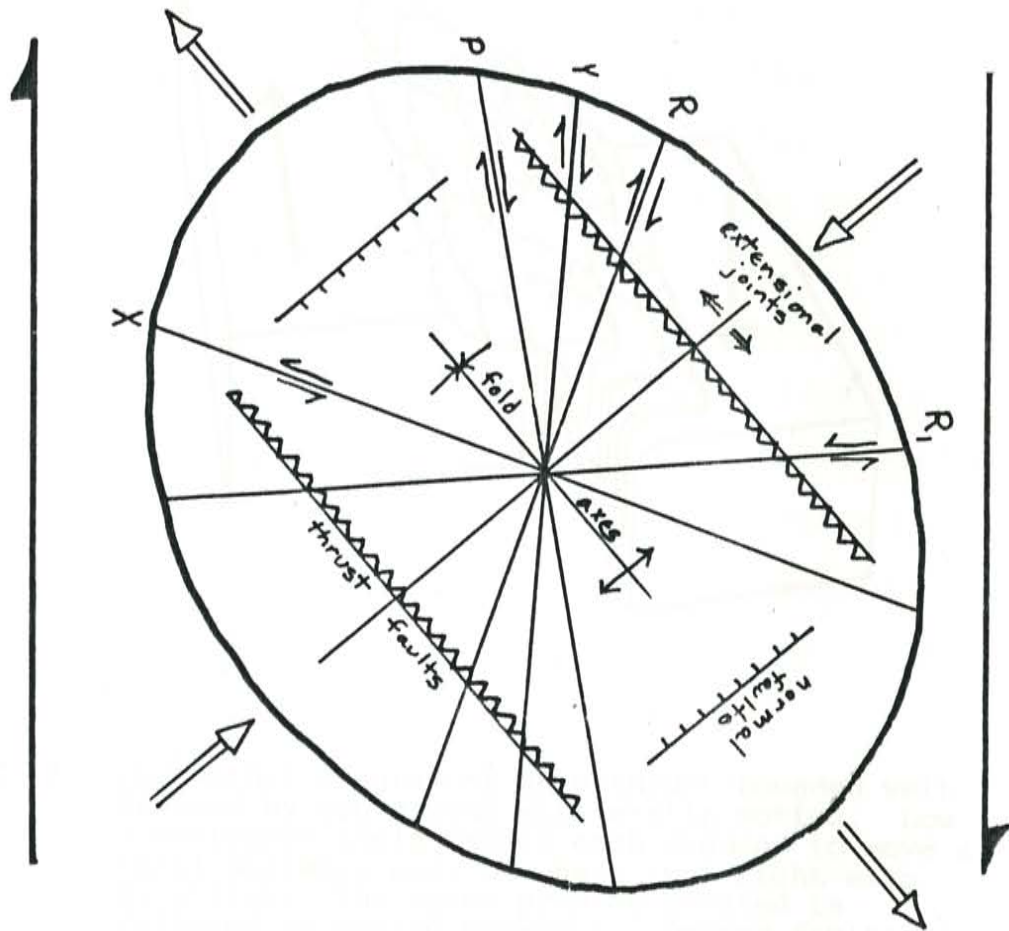


FIGURE 28: Strain ellipse in a right-lateral wrench regime: R, P, Y: synthetic wrench faults and wrench zone R1, X: antithetic strike-slip faults. Fold axes in direction of elongation of strain ellipse. From Hancock, 1985, "loosely after Harding, 1974."

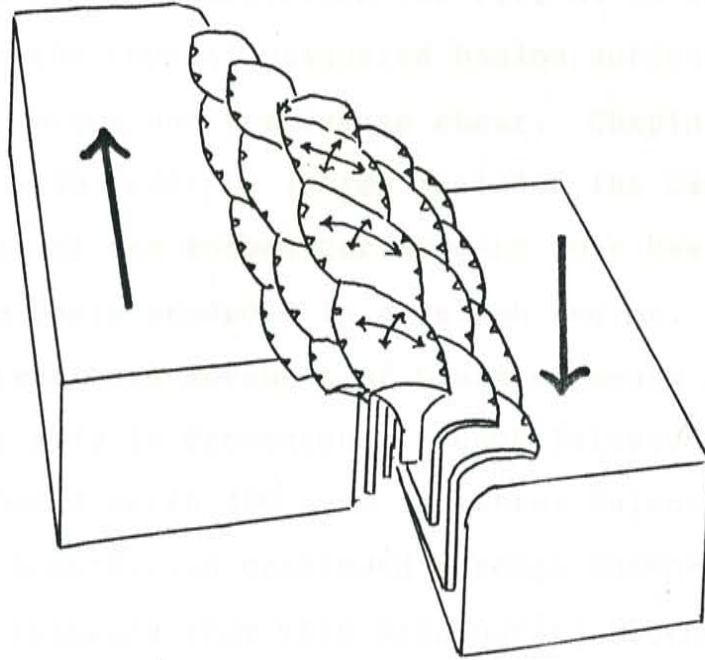


FIGURE 29: Conceptual diagram of an upthrust-bounded welt created by convergent strike-slip motion. Low convergence angle causes each segment to move a small distance past the next in a right-slip direction. The space problem created is relieved by upward movement. Deeper faults may tend to coalesce and braid, rather than be parallel, and the upthrusts are not necessarily so symmetrically disposed as is shown. From Lowell, 1972, figure 9, p. 3099.

adjacent uplifts. Transtensional wrench movement develops features which appear extensional. The scale of the Rio Grande rift is larger than typical rhomb grabens, and Freund (1982) identifies it as a genuine extensional rift. Chapin (1979), however, describes the rift as an echelon openings, with the ends of staggered basins subjected to scissors-like torque and transverse shear. Chapin and Cather (1981) also describe (which includes the Cañoncito de la Uva area) of the Eocene Carthage-La Joya basin, an Echo Park type basin produced in a wrench regime. They document compressional movement of plate elements along an east-northeast axis in Cretaceous through Paleocene time, and a shift toward north 45° east in latest Paleocene time. Northeastward compression continued through Eocene time. Sedimentation westward from this area during Eocene time shows there was uplift at this time (Chapin and Cather, 1981).

A COCORP seismic line (Fig. 30) through Abo Pass shows a deep, planar subvertical structure is present near the front of the Los Piños Mountains, and buried high-standing blocks in the basin west of them (Brown and others, 1979). The blocks are suggestive of the blocks envisioned by Crowell (1974) forming as the late Cenozoic basins of southern California developed along the San Andreas fault.

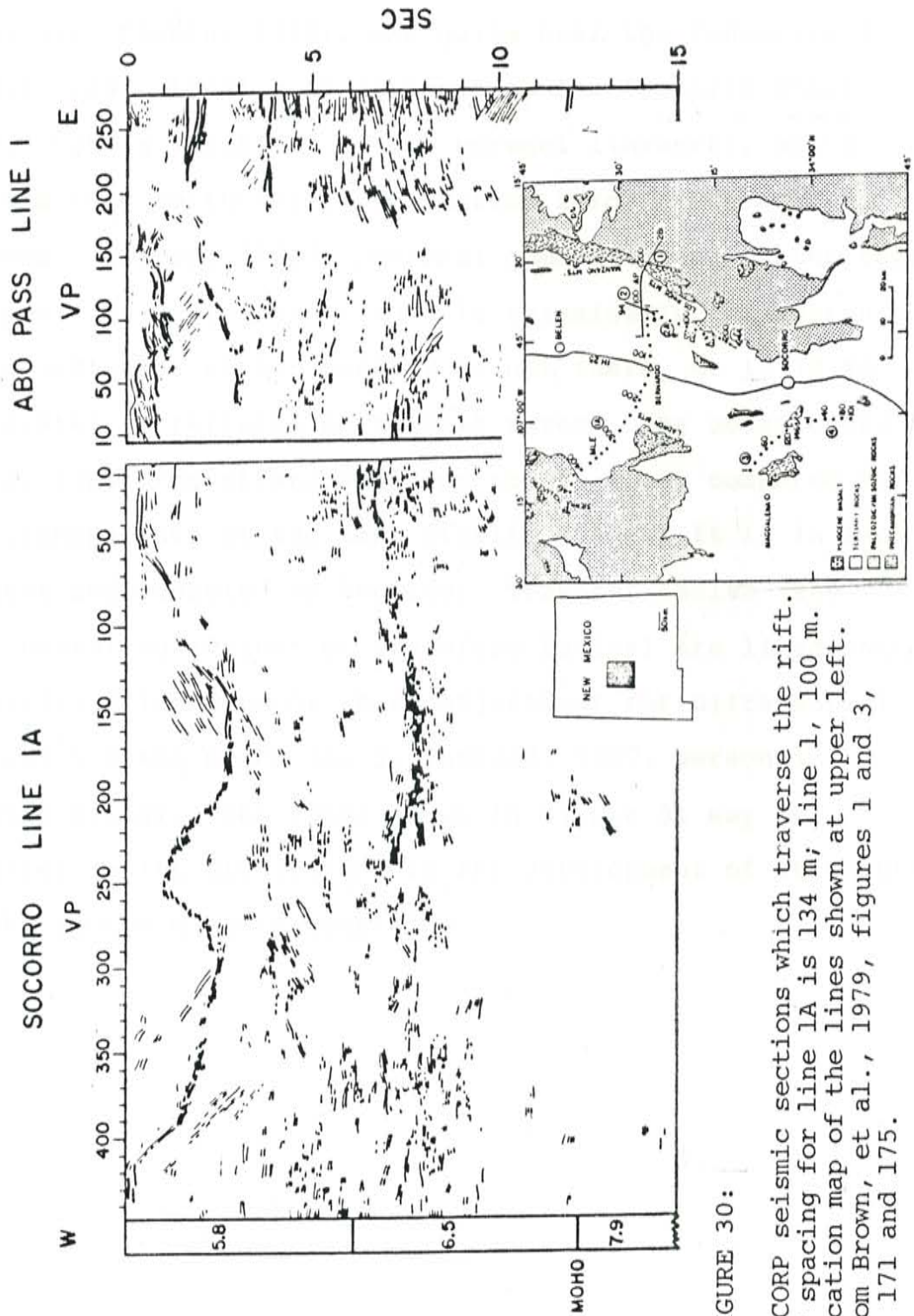


FIGURE 30:

COCORP seismic sections which traverse the rift. VP spacing for line IA is 134 m; line I, 100 m. Location map of the lines shown at upper left. From Brown, et al., 1979, figures 1 and 3, p. 171 and 175.

Several parallel lineaments cross the Rio Grande rift (Fig. 31; Chapin, 1978), one quite near the Cañoncito de la Uva area. Locally it is known as the "Socorro shear zone," but is identical to the Morenci lineament, which extends from northeastern New Mexico through Morenci, Arizona. Sanford (1987, personal communication) notes that the position of the shear zone is seismically transparent; which indicates either that it is not there, or it is so brecciated it reflects no seismic waves. The conspicuous reflections from strata adjacent to the zone, compared to the transparency of the zone itself, suggest it is in fact present and occupied by breccia. Transfer faults (the continental equivalent of transform faults) are lineaments of strike-slip movement where adjustment for differential extension takes place (A. J. Tankard, 1987, personal communication). The zones shown in figure 31 may be transfer faults significant to the development of structure in the southern Rocky Mountains.

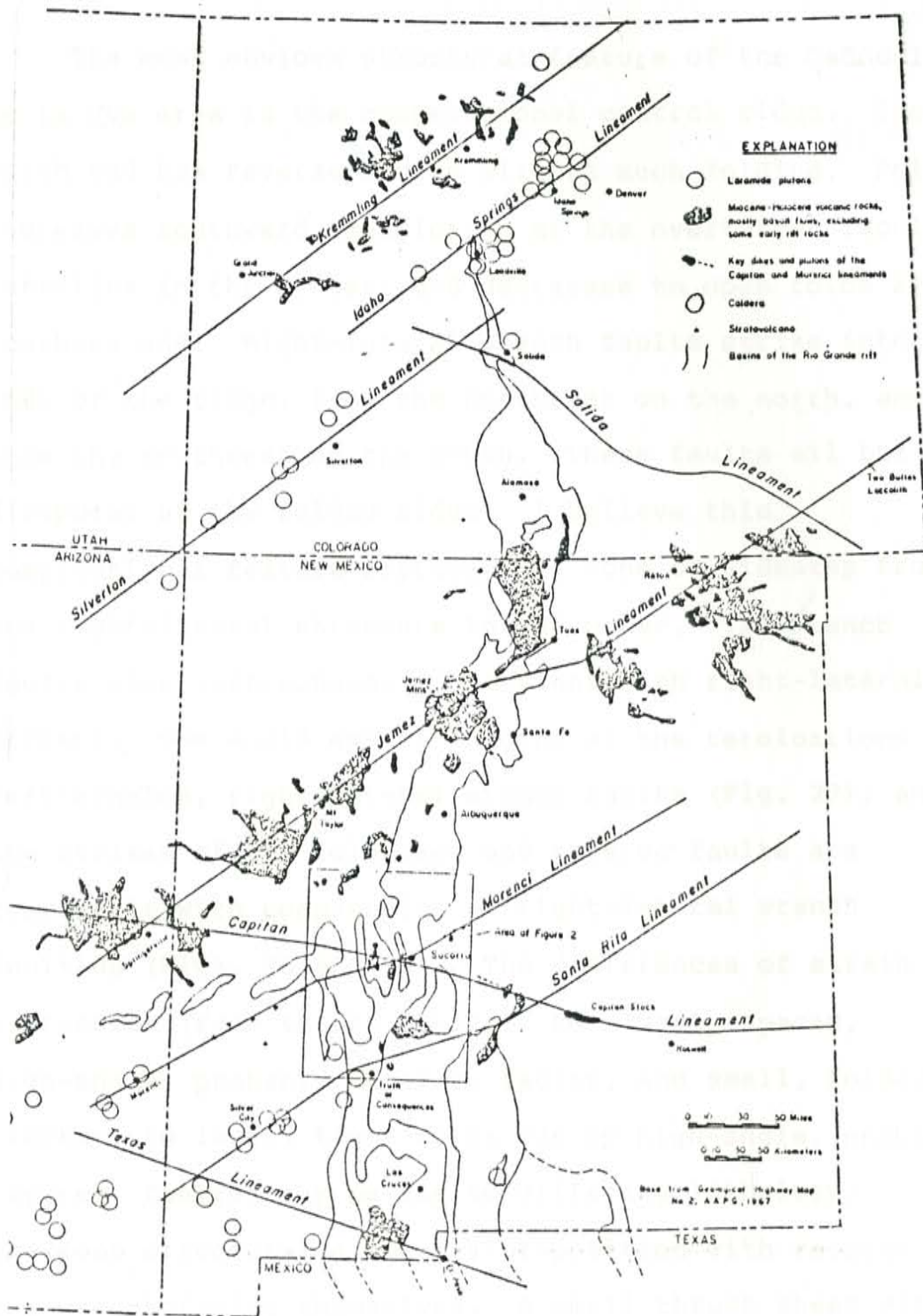


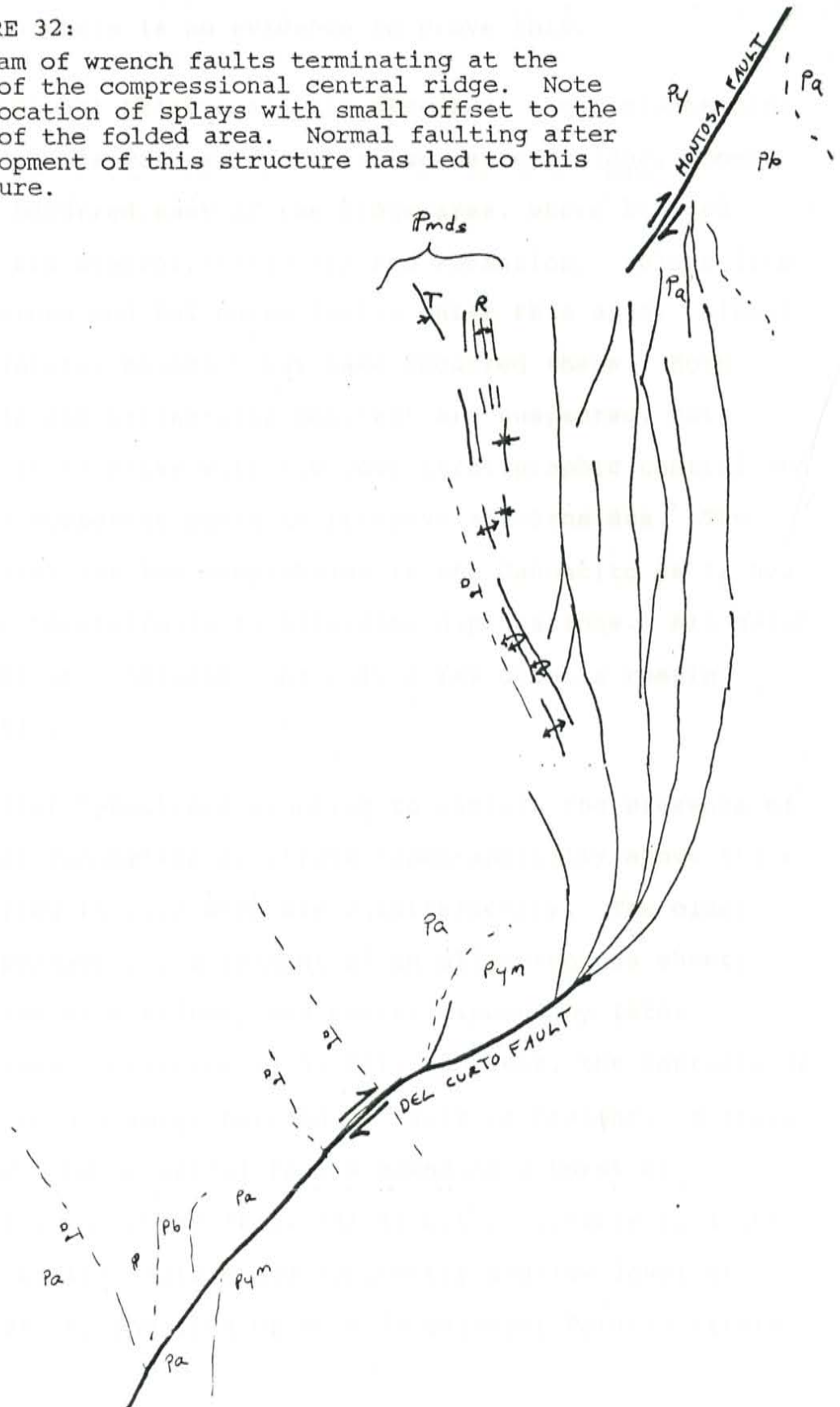
FIGURE 31: Generalized map of the Rio Grande rift and major crustal lineaments. From Chapin, et al., 1978, figure 1, p. 114.

Structural Discussion

The most obvious structural feature of the Cañoncito de la Uva area is the compressional central ridge. The north end has reverse faults without much folding. Folding increases southward, culminates at the overturned isoclinal anticline in the center, and decreases to open folds at the southern end. Right-lateral wrench faults strike into the ends of the ridge, from the northeast on the north, and from the southwest on the south. These faults all but disappear at the folded ridge. I believe this compressional feature represents a zone of sidestep from one right-lateral structure to the other. The wrench faults step left-echelon (consistent with right-lateral offset). One would expect folding at the terminations of left-echelon, right-lateral wrench faults (Fig. 27), and the strikes of the fold axes and reverse faults are compatible with compression of right-lateral wrench faulting (Figs. 28 and 32). The differences of strain expression (from thrust faults; to closely-spaced, high-angle, probably reverse, faults, and small, folded blocks; to large, tight folds cut by high-angle, probably reverse, faults) may be due to differing lithology, previous structural elements, or position with respect to the wrench faults themselves. A small thrust sheet with imbricate splays (Fig. 23) neatly explains the local structure at the contact between the Moya Formation and the Bursum Formation in the northeast corner of section 15,

FIGURE 32:

Diagram of wrench faults terminating at the ends of the compressional central ridge. Note the location of splays with small offset to the east of the folded area. Normal faulting after development of this structure has led to this exposure.



although there is no evidence to prove this.

I do not believe all the stress of the side-stepping wrench faults was expressed in the central ridge. Some strain occurred east of the ridge area, where braided faults are present within the Abo Formation. Splays from the Montosa and Del Curto faults enter this area. Direct right-lateral movement may have occurred there. Both dip-slip and strike-slip movement are suspected, but difficult to prove with the poor stratigraphic control and lack of competent rocks to preserve slickensides. The hypotheses for the compression in the Cañoncito de la Uva area are preferable to alternate explanations. All major features are included, and only a few details remain enigmatic.

Other hypotheses existing to explain the presence of vertical Pennsylvanian strata topographically above the flat-lying Permian beds are unsatisfactory. The older rocks perhaps are a remnant of an allochthonous sheet, preserved as a klippe, and better exposed by later extensional tectonics (Fig. 33). However, the contacts do not suggest a large horizontal fault is present. Extreme drag-folding on normal faults bounding a horst of Pennsylvanian rocks (Fig. 34) is not reasonable in light of the brittle nature and apparently shallow level of deformation, and lack of drag in adjacent Permian strata.

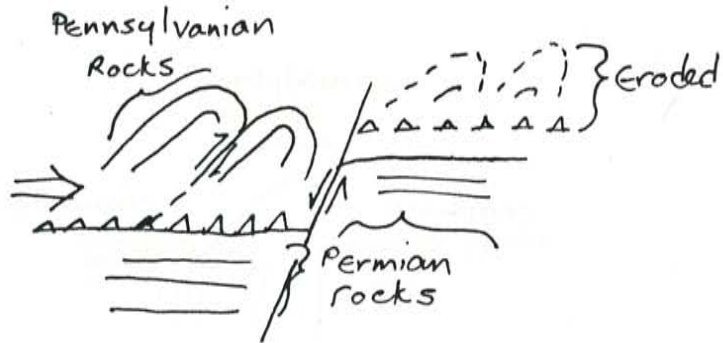


FIGURE 33: Possible allochthonous origin of the central compressional ridge.



FIGURE 34: Horst interpretation of the central ridge.

This compression is related to the pre-rift tectonic movement in the Rio Grande rift area. From the Manzano Mountains southward, the Montosa fault exhibits many features of wrench faults (differential offset along strike, major sub-parallel splays, change of dip direction along strike, change of apparently-downthrown side). There is documentation of true reverse movement along this zone near Abo Pass (Stark and Dapples, 1946). But in central Socorro County it has been shown to have right-lateral offset (Colpitts, 1986). Basement-cored uplifts to the south (Seager and others, 1986) and southwest (Drewes, 1982) have some oblique movement. Figure 35 shows possible regional movement on the Montosa fault from Abo Pass to south of the Cañoncito de la Uva area. Wrench to oblique movement dominated where the Montosa fault strikes northeasterly, and movement closer to true reverse occurred where it strikes northward. The regional relationship is suggestive of a positive flower structure in both style and scale of deformation. Compressive forces in this area during Laramide time initially were directed east-northeast, and later shifted to northeast (Chapin and Cather, 1981). This shift in stress orientation may also be responsible for some difference in character of movement on the Montosa fault from north to south.

Extensional faulting related to rift opening postdates and complicates the wrench-compression fault pattern. In the Cañoncito de la Uva area, two major extensional fault

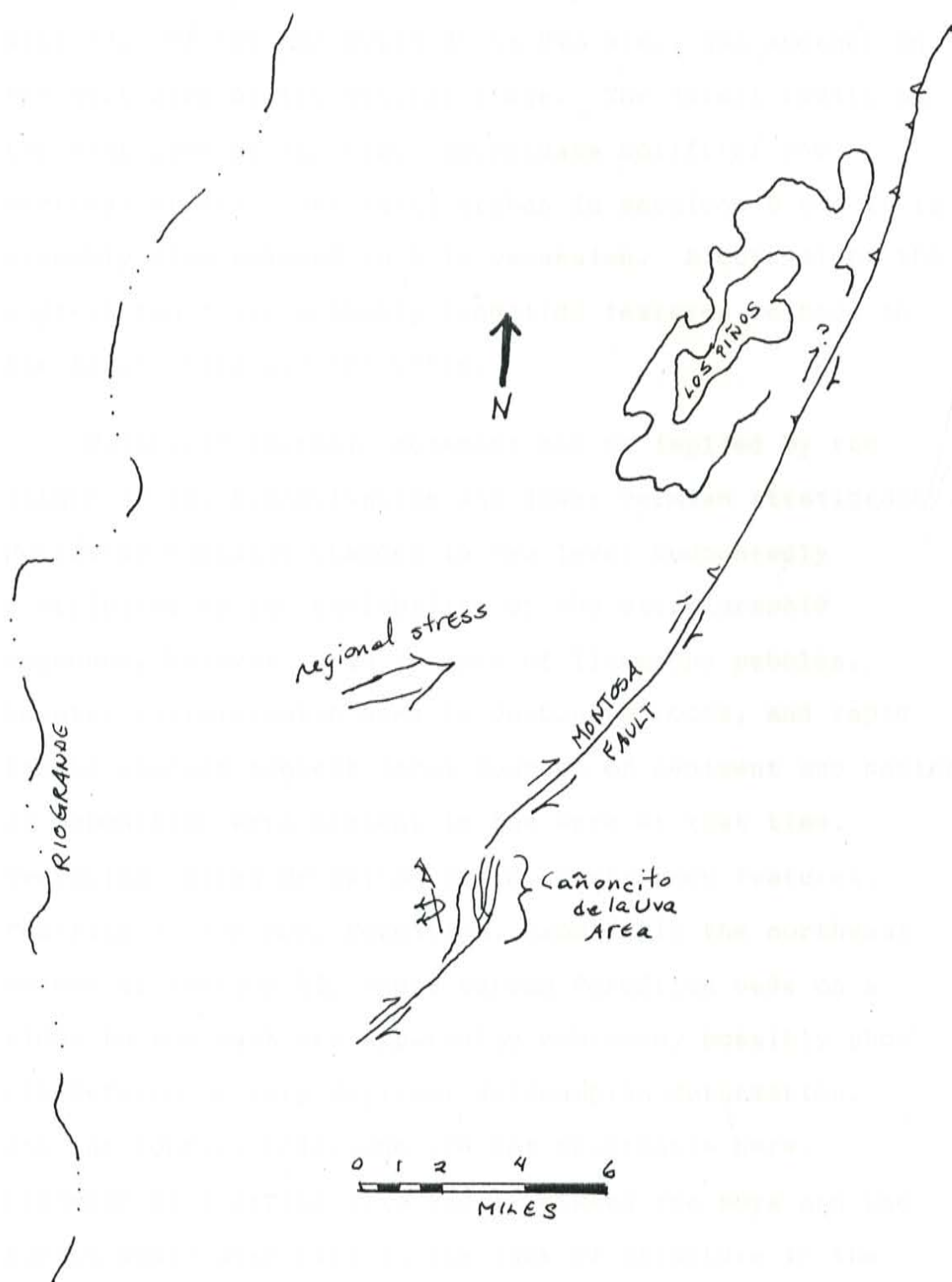


FIGURE 35: Diagram of possible regional relations from Abo Pass, southward through Cañoncito de la Uva area.

sets, downdropped to the west, are present: one on the west edge of the Cañoncito de la Uva area, and another on the west side of the central ridge. The normal faults on the west side of the ridge accentuate uplift of the vertical strata. The small graben in sections 9 and 16 is probably also related to this extension. Blocks along the western fault are probably landslide features related to the large scarp present there.

Paleozoic tectonic movement may be implied by the nature of the Pennsylvanian and lower Permian stratigraphy. Worldwide eustatic changes in sea level undoubtedly contributed to the variability of the stratigraphic sequence, however large volumes of limestone pebbles, angular siliciclastic sand in carbonate rocks, and rapid facies changes suggest local sources of sediment and basins of deposition were present in the area at that time. Tectonism during deposition could create such features. Faulting in the Moya Formation, exposed in the northeast corner of section 15, where Bursum Formation beds on a ridge to the east are apparently unbroken, possibly show pre-Permian or very earliest Wolfcampian deformation. Angular contact relations are not observable here. Presence of a strike-slip fault between the Moya and the Bursum would also explain the lack of structure in the Bursum, but such a fault has not been located. Some or most of the northeast striking faults in Pennsylvanian rocks in the west side of the Cañoncito de la Uva area may

also be of this age. Reactivation of these structures at later times is likely.

"Flat faults" (a misnomer, field term, applied to east-dipping planar elements) are not present within the Cañoncito de la Uva area, but are exposed all around it. These faults occur most commonly below the Glorietta and Joyita Sandstones (for example, see Bauch, 1982, Colpitts, 1986), where strata are remarkably incompetent. The possibility of a genetic relationship of flat-faults to wrench faults was discussed with Dr. Charles Chapin. Perhaps flat faults sole small sheets of strata caught by rocks across a wrench fault, and lateral movement takes place on horizontal surfaces in highly incompetent strata. Sheets on one side of the wrench fault are dragged along by the other block. The spatial relationship of these two fault types could be important, and mapping may support or eliminate the hypothesis of a genetic relationship. Dr. Chapin suggested physical modelling of wrench faults in highly stratified material may also add insight regarding flat faults.

APPENDIX OF TABLES

TABLE 1

DESCRIPTION OF THIN SECTIONS

Location of thin sections is noted on stratigraphic plates.

NUMBER	FORMATION	PLATE
-----	-----	-----
1-13	Burrego	7
14-16	Story	8
17-18	Del Cuerto	8
19-26	Moya	8
27-33	Moya	10
34-41	Moya	9
42-49	Bursum	11
50-60	Abo	12

IS#	Grain %				carbo-nate	Intergranular %				Fossil type				Texture										
	quartz	fldspr	mica	lithic		opaque	biota	oolid	peloid	intrcl	silica	cal-cite	lime mud	matrix	clay/mica	brachpd	crinoid	bryozoa	foram	shell fragment	other	size distribution	grain shape	type of support
1	30	4	1	2	Ø 40					20		3	3								coarse silt to med. sand	angular	grain matrix	fibrous veins
2	32	4	14	Ø 2						✓		48	48								v.f. silt to v.f. sand	subangl.	grain	grains aligned, sutured contacts
3	47	6	→ 24	Ø 2						5											silt and clay	subangl.	grain	mainly opegaetram
4	28	5	2	7	4	2				5											v.f. sand to f. pebble	subangl.	grain	feet pair highly altered
5					25 ?					2	7	3									clay to f. pebble	broken	grain matrix	bedded, upright geopetal
6	28	3	2	Ø 4						3		30	30								f.s. silt to f. sand	rounded	grain matrix	bedded via qtz. amnt.
7	17	Ø < 1	Ø 14							4		64	64								m. silt to v.f. sand	subangr	matrix	septarian nodule
8	30	45	3	3	< 1	8				5		2	2								c. silt to m. sand	subangr	grain	feld. adt. to matrix
9	30	45	tr	Ø 10						5		10	10								v.f. sand to m. sand	broken	matrix	hematite common
10					12					10	58/20										to 2 mm	broken	matrix	grains parallel to bedding, opaque streaks
11					65					5	30										to 2.5 mm	broken	grain	upright geopetals, chert
12	35	45	tr	Ø 10						7		10	10								c. silt to m. sand	angular	grain	grain coated
13	40	35	2	Ø 15							15/20	tr	tr								c. silt to m. sand	angular	grain	styloites w/dark stain
14					40		15				15/20										to 3 mm	broken work	grain	styloites w/dark stain
15					35		15			11	65										to 4 mm	broken	grain	spar-filled fractures
16					35		15				0/50												grain	
17	41	35	2	Ø 25			4			2		1	1								c. silt to f. sand	subangl.	grain	crossbedded
18	15	3			5		35			42	0/30										c. silt to m. sand	subangl.	grain	grain
19					35		35														to 3 mm	broken	grain	styloites w/dark stain
20					35		*														to 3 mm	broken	grain and matrix	re crystallized styloites w/dark stain patchy bco of intracryst boundaries

TS#	Grain %		carbo- nate	Intergranular %			Fossil type					Texture size distribution	grain shape	type of support	other
	clastic fldspr quartz	opaque fossil lithic mica		silica	cal- cite	lime mud	clay/ mica	brachpd	crinoid	bryozoa	foram				
21		65			0/35		✓	✓				to 5 mm	broken	grain	near stallaged chert coat of sty folites w/ to. own stain
22		23		12	65		10	15	75			to 4 mm	broken	matrix	near stallaged, dis- chert, chert geopetal str.
23		25	15	10	50		10	15	30	45		to 5 mm	whole and broken	grain	
24		25	20	10	45		30		70			to 10 mm	whole	grain	irregular spar-filled pores
25		7		3	70		100		100	J		to 0.5 mm	broken	matrix	buried structures spar-filled fractures
26		20		5	75		100		100			to 8 mm	whole & broken	grain	textured, spar-filled geopetal; minute + sp.
27		65		5	25/5		✓	✓				to 4 mm	broken	grain	sty folite w/ dark stain geopetal, upright textured. fossils
28		25	*	5	75		50	15	35	P			broken	grain	only intracrystals described this lith. dark stained sty folites
29	18 20 q φ	15 7	40	✓			✓					c. silt to f. sand	broken subangl.	matrix	feldspar, altered fossils, intracrystals bedded sand/cgl
30	45 30 φ	15 φ	7	✓			✓	✓				f. sand to v.f. pebble	subground	grain	dischordant geopetal black staining grain boundaries
31		25	15	5	55		✓	✓				to 0.5 mm	broken	grain	
32		80		20			25	65	10			to 4 mm	broken	grain	
33		45			55		60	20	20	P _m			broken	grain	sty folites w/ dark stain, texture of fossils, minor disint.
34		30		5	65		95	5				to 2 mm	broken	matrix	dischordant geopetal easily stain, rexten.
35	50 45 φ + φ	φ	60	1			15	75	5	5		m. sand tr f. pebbles	subangl.	grain	dark staining grain boundaries, f.e.a.t.
36		60	5		30		15	75	5	5		to 3 mm	broken	grain	spar-filled fractures

IS#	Grain %		carbo- nate	Intergranular %				Fossil type		Texture		grain shape	type of support	other	
	clastic lithic mica fldspr quartz	opaque fossil		silica	cal- cite	lime mud	clay/ mica	brachpd	crinoid	trilobite	shell fragment				size distribution
37			60		10	0/30		8	70	20	to 13 mm	broken	grain	upright geopetal, stylolite w/ dark stain some fossils micritized	
38			35		35			10	50	35	to 7 mm	whole & broken	grain	stylolites, dischordant geopetal, n. n. n.	
39			40		25/30			✓	✓	✓	to 5 mm	broken	grain	coated grains bedded, stained stylol.	
40			60		5	35		25	35	5	to 4 mm	broken	grain	coated grains bedded, stained stylol.	
41			60	15		0/25		25	15	50	to 6 mm (intraclast to 3 cm.)	broken	grain	coated grains stained stylolites	
42		8					5				m.silt to v.f.sand	subangl.	grain	bedded, fs. altered	
43		5									m.silt to m.sand	subangl.	grain	crudely bedded	
44			98		2	✓	4	✓	✓	✓	intraclasts to 2 cm	rounded	grain	stylolites w/ dark stain, calcite veinlets	
45		30			2			✓			m.silt to v.f.sand	subangl.	grain	significant alteration	
46		10					3				m.silt to v.f.sand to 8 mm	subangl.	grain	crossbedded on comp.	
47			80		0/20			3	4	30	to 8 mm	broken	grain	other 50% biotas as coatings on grains	
48		5			30			✓	✓	✓	v.f.sand to m.sand	subangl.	grain	crudely bedded	
49		10			15		✓	5	5	70	n.sand to f. pebble to 2 mm	angular	grain	iron stained	
50			30		20			5	5	20	to 2 mm	broken	grain	coated grains fossils n. n. n.	
51			5		95			?	100		to 0.1 mm	broken	matrix	dark, purple sh str- eak on fractures	
52		7					93				v.f.silt to c.silt	angular	matrix	cumulate red stain	
53		7					37				clay to c.silt	subangl.	matrix and grain	matrix	cumulate red stain
54		60			2		30				clay to v.f.sand	subangl.	matrix	matrix	spar-filled pebbles
55		6			?		55				clay to c.silt	subangl.	matrix	matrix	bedded on grain
56		7			2		17				m.silt to c.sand	rounded	grain	bedded on grain	
57		10			5		40				clay to c.silt	rounded	grain	massive calcite patches to 3 mm bleached zones	

IS#	Grain %		carbo- nate	Intergranular %			Fossil type	Texture size distribution	grain shape	type of support	other
	clastic	opaque		silica	cal- cite	matrix					
58	10	1	0	65	?	4		v.f. sand to c. pebble	rounded	grain	lithics mostly siltstone
59	65	20		6		3		f.silt to c.silt	subangl.	grain	
60	70	tr		8		tr		clay to v.f. sand	subangl.	grain	bedded on composition

TABLE 2

ATTITUDES OF FAULT PLANES

ATTITUDE	SECTION	CLASS	FORMATION
227/51 SE	9	IV	Pb, PPM
42/71 NW	9	IV	Pb
60/85 NW	9	IV	Pb
169/80 E	10	II	Pb
164/76 E	10	II	Pb
334/29 W	10	II	PPM
138/11 NE	10	II-R	PPM
10/90	10	II	PPM
356/90	10	II	PPM
330/44 SW	10	II	PPM
346/60 SW	10	II	PPM
193/10 E	11	I-M	Pa, Pb
234/75 E	11	I-M	Pym, Pa
26/80 NW	11	I-M	Pb
352/16 W	12	I	Pb
176/31 E	12	I	Pb
200/31 E	12	I	Pb
246/57 E	12	IV	Pb
184/64 E	13	I	Pa/u
24/75 W	13	I	Pa/u
17/58 W	13	V	Pyt
162/62 E	15	II	PPM
1/46 W	15	II	PPM
72/45 N	15	IV	PPM
153/75 NE	16	III	Pb, PPdc
145/57 NE	16	III	PPM
66/45 NW	21	IV	PPM
59/45 NW	21	IV	PPM
346/75 SW	22	II	Pb, PPbg
39/58 NW	23	I/II	Pa
330/60 SW	23	I	Pa
341/78 SW	23	I	Pa
353/55 SW	23	I	Pym
334/50 SW	23	I	Pa
354/31 W	23	II	PPM
316/85 SW	23	II	Pb, PPM
341/36 SW	24	V	Pyt
319/8 SW	24	V/I	Pym
185/43 E	24	I	Pym, Pa

Class designation

- I) Braided faults on eastern side of area
(M) indicates on trace of Montosa fault
- II) At tight fold in center of area
(R) indicates known reverse movement
- III) Northeast striking, usually with small offset
- IV) Major faults in western limestone province
- V) Along probable thrust in southeast part of area

TABLE 3

TREND AND PLUNGE OF FOLD AXES

LOCATION	TREND (AZ)	PLUNGE
s. 10	123	18
11	240	1
11	9	1
11	8	5
11	22	9
12	358	6
12	359	5
12	348	1
12	67	24
13	185	6
14	167	1
14	274	7
15	89	12
15	343	1
23	194	9
23	339	2
24	53	4
24	187	29
24	174	6

REFERENCES CITED

- Altares, T., 1985, Bursum formation in central New Mexico: New Mexico Institute of Mining and Technology Thesis (M. S.), in progress.
- Bates, R. L., R. H. Wilpolt, A. J. MacAlpin, and G. Vorbes, 1947, Geology of the Gran Quivira quadrangle, New Mexico: New Mexico Bureau of Mines and Mineral Resources, Bulletin 26, 52 p.
- Bauch, J.H.A., 1982, Geology of the central area of the Loma de las Canes quadrangle, Socorro County, New Mexico: New Mexico Institute of Mining and Technology Thesis (M. S.), 116 p.
- Boyer, S. E., and Elliott, D., 1982, Thrust systems: American Association of Petroleum Geologists Bulletin, v. 66, p. 1196-1230.
- Brown, L. D., P. A. Krumhansl, C. E. Chapin, A. R. Sanford, F. A. Cook, S. Kaufman, F. E. Oliver, Fk. S. Schilt, 1979, COCORP seismic reflection studies of the Rio Grande Rift: p. 169-184 in Rio Grande Rift: Tectonics and Magmatism, R. E. Riecker, (ed.), American Geophysical Union, Washington, D. C., 438 p.
- Chapin, C. E., R. M. Chamberlin, G. R. Osburn, D. W. White, and A. R. Sanford, 1978, Exploration framework of the Socorro geothermal area, New Mexico: New Mexico Bureau of Mines and Mineral Resources Special Publication no. 7, p. 115-127.
- Chapin, C. E., 1979, Evolution of the Rio Grande Rift -- a summary: p. 1-5 in Rio Grande Rift: Tectonics and Magmatism, R. E. Riecher, ed., American Geophysical Union, Washington D. C., 445 p.
- Chapin C. E., and Cather, S. M., 1983, Eocene tectonics and sedimentation in the Colorado Plateau--Rocky Mountain Area: Rocky Mountain Association of Geologists, p. 33-56.
- Colpitts, R. M., 1986, Geology of the Sierra de la Cruz area: New Mexico Institute of Mining and Technology Thesis (M. S.), 108 p.
- Crowell, J. C., 1974, Origin of Late Cenozoic basins in southern California: p. 190-204 in Tectonics and sedimentation, W. R. Dickinson (ed.), Society of Economic Paleontologists and Mineralogists Special Publication 22, 204 p.

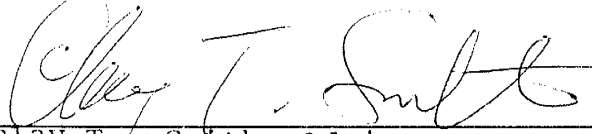
- Darton, N. H., 1922, Geologic structure of parts of New Mexico: United States Geological Survey Bulletin 726, p. 173-275.
- Dibblee, T. W., Jr., 1977, Strike-slip tectonics of the San Andreas fault and its role in Cenozoic basin evolution: p. 26-38 in Late Mesozoic and Cenozoic Sedimentation and tectonics in California: San Joaquin Geological Society.
- Drewes, H., 1982, Some general features of the El Paso-Wickenburg transect of the Cordilleran orogenic belt, Texas to Arizona: p. 882-892 in Geologic studies of the Cordilleran thrust belt, R. B. Powers, ed.: Rocky Mountain Association of Geologists, Denver, CO, 976 p.
- Freund, R., 1982, The role of shear in rifting: p. 33-39, in Continental and Oceanic Rifts, G. Palmason (ed.); Geodynamic Series, v. 8, American Geophysical Union, Geological Society of America, 309 p.
- Hafner, W., 1958, Faulting associated with differential vertical uplift and with horizontal compression (upthrust faults versus overthrust faults): Shell Oil Company, Exploration and Production, New York, 16 p.
- Hancock, P. L., 1985, Brittle microtectonics: principles and practice: Journal of Structural Geology, v. 7, p. 437-457.
- Harding, T. P., 1974, Petroleum traps associated with wrench faults: American Association of Petroleum Geologists Bulletin, v. 58, p. 1290-1304.
- Harding, T. P., 1985, Seismic Characteristics and identification of negative flower structures, positive flower structures, and positive structural inversion, American Association of Petroleum Geologists Bulletin, v. 69, p. 582-600.
- Harland, W. B., 1971, Tectonic transpression in Caledonian Spitzbergen: Geological Magazine, v. 108, p. 27-41.
- Hunt, A., 1983, Plant fossils and lithostratigraphy of the Abo Formation (Lower Permian) in the Socorro area and plant biostratigraphy of Abo red beds in New Mexico: New Mexico Geological Society Guidebook, 34th Field Conference, Socorro Region II, p. 157-163.
- Jicha, H. L., Jr., and C. Lochman-Balk, 1958, Lexicon of New Mexico geologic names: Precambrian through Paleozoic: New Mexico Bureau of Mines and Mineral Resources, Bulletin 61, 137 p.

- Kingma, J. T., 1958, Possible origin of piercement structures, local unconformities and secondary basins in the Eastern Geosyncline, New Zealand: *New Zealand Journal of Geology and Geophysics*, v. 1, p. 269-274.
- Kottlowski, F. E., R. H. Flower, M. L. Thompson, and R. W. Foster, 1956, Stratigraphic studies of the San Andres Mountains, New Mexico: *New Mexico Bureau of Mines and Mineral Resources, Memoir 1*, 132 p.
- Kottlowski, F. E., 1963, Paleozoic and Mesozoic strata of central and southwestern New Mexico: *New Mexico Bureau of Mines and Mineral Resources Bulletin 79*, 100 p.
- Kottlowski, F. E., and W. J. Stewart, 1970, The Wolfcampian Joyita uplift in central New Mexico: *New Mexico Bureau of Mines and Mineral Resources, Memoir 23*, p. 1-31.
- Lee, W. T., and G. H. Girty, 1909, The Manzano Group of the Rio Grande valley, New Mexico: *United States Geological Survey Bulletin 389*, 141 p.
- Lowell, J. D., 1972, Spitsbergen Tertiary orogenic belt and Spitsbergen fracture zone: *Geological Society of America Bulletin*, v. 83, p. 2091-3101.
- Maulsby, J., 1981, Geology of the Rancho de Lopez area east of Socorro, New Mexico: *New Mexico Institute of Mining and Technology Thesis (M.S.)*, 83 p.
- Moody, J. D., 1973, Petroleum exploration aspects of wrench-fault tectonics: *American Association of Petroleum Geologists Bulletin*, v. 57, p. 449-476.
- Needham, C. E., and Bates, R. L., 1943, Permian type sections in central New Mexico: *Geological Society of America Bulletin*, v. 54, p. 1653-1668.
- Quenell, A. M., 1958, The structural and geomorphic evolution of the Dead Sea Rift: *Quarterly Journal of the Geological Society of London*, v. 114, p. 1-24.
- Reading, H. G., 1980, Characteristics and recognition of strike-slip fault systems: p. 7-26 in *Sedimentation in oblique-slip mobile zones*, P. F. Ballance and H. G. Reading, eds.: *Special Publication of the International Association of Sedimentologists*, v. 4, 265 p.
- Rejas, A., 1965, Geology of the Cerro de Amado Area, Socorro County, New Mexico: *New Mexico Institute of Mining and Technology Thesis (M. S.)*, 128 p.
- Seager, W. R., 1983, Laramide wrench faults, basement-cored uplifts, and complimentary basins in southern New Mexico: *New Mexico Geology*, v. 5, p. 67-76.

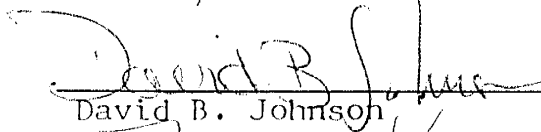
- Seager, W. R., G. H. Mack, M. S. Raimonde, and R. G. Ryan, 1986, Laramide basement-cored uplifts and basins in south-central New Mexico: p. 123-130 in New Mexico Geological Society, 37th Field Conference-Truth or Consequences Region, 317 p.
- Smith, C. T., 1983, Structural problems along the east side of the Socorro constriction, Rio Grande Rift: New Mexico Geological Society Guidebook, 34th Field Conference, Socorro Region II, p. 103-109.
- Sporli, K. B., 1980, New Zealand and oblique-slip margins: tectonic development up to and during the Cainozoic: p. 147-170 in Sedimentation in oblique-slip mobile zones, P. F. Ballance, H. G. Reading, eds.: Special Publication of the International Association of Sedimentologists, v. 4, 265 p.
- Stark, J. T., and E. C. Dapples, 1946, Geology of the Los Pinos Mountains, New Mexico: Geological Society of America Bulletin, v. 57, p. 1121-1172.
- Sylvester, A. G., and Smith, R. R., 1976, Tectonic transpression and basement-controlled deformation in San Andreas Fault Zone, Salton Trough, California, American Association of Petroleum Geologists Bulletin, v. 60, no. 12.
- Thompson, M. L., 1942, Pennsylvanian system in New Mexico: New Mexico Bureau of Mines and Mineral Resources Bulletin No. 17
- Wernicke, B., and B. C. Burchfiel. 1982, Modes of extensional tectonics: Journal of Structural Geology, v. 4, p. 105-115.
- Wilcox, R. E., T. P. Harding, and D. R. Seely, 1973, Basic wrench tectonics: American Association of Petroleum Geologists Bulletin, v. 57, p. 74-96.
- Wilpolt, R. H., A. J. MacAlpin, R. L. Bates, and G. Vorbe, 1946, Geologic map and stratigraphic sections of Paleozoic rocks of Joyita Hills, Los Pinos Mountains, and northern Chupadera Mesa, Valencia, Torrance and Socorro Counties, New Mexico: United States Geological Survey Oil and Gas Investigations, Preliminary Map 61.
- Wilpolt, R. H., and A. A. Wanek, 1951, Geology of the region from Socorro and San Antonio east to Chupadera Mesa, Socorro County, New Mexico: United States Geological Survey Oil and Gas Investigations Map OM-121.

Wood, G. H., and S. A. Northrup, 1946, Geology of the Nacimiento Mountains, San Pedro Mountain and adjacent plateaus in parts of Sandoval and Rio Arriba Counties, New Mexico: United States Geological Survey Oil and Gas Inventory Map 57.

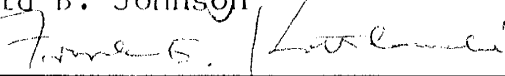
This thesis is accepted on behalf of the faculty
of the Institute by the following committee:



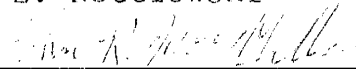
Clay T. Smith Advisor



David B. Johnson



Frank E. Kottlowski



John Macmillan

April 30, 1987

Date